Late Neoproterozoic–Cambrian magmatism in Dronning Maud Land (East Antarctica): U–Pb zircon geochronology, isotope geochemistry and implications for Gondwana assembly

Cheng-Cheng Wang[a*], Joachim Jacobs[a], Marlina A. Elburg[b], Andreas Läufer[c], Synnøve Elvevold[d]

[a] Department of Earth Science, University of Bergen, PB7803, N-5020 Bergen, Norway

[b] Department of Geology, University of Johannesburg, Auckland Park 2006, Johannesburg, South Africa

[c] Federal Institute for Geosciences and Natural Resources (BGR), Stilleweg 2, 30655, Hannover, Germany

[d] Norwegian Polar Institute, Tromsø, Norway

Corresponding email: Cheng-Cheng.Wang@uib.no

Declarations of interest: none

Abstract

Dronning Maud Land (DML) is a key area for the better understanding of the geotectonic history and amalgamation processes of the southern part of Gondwana. Here, we present comprehensive new zircon U–Pb–Hf–O, whole-rock Sm–Nd isotopic and geochemical data for late Neoproterozoic-Cambrian igneous rocks along a profile from central to eastern DML, which provides new insights into the crustal evolution and tectonics of the region. In central DML, magmatism dominantly occurred at 530–485 Ma, with 650–600 Ma charnockite and anorthosite locally distributed at its eastern periphery. In contrast, eastern DML experienced long-term and continuous granitic magmatism from ca. 650 Ma to 500 Ma. In central DML, the 650–600 Ma samples are characterized by highly elevated $\delta^{18}O$ (7.5–9.5 ‰), associated with slightly negative to positive εHf values (-1–+3), indicating significant addition of high-$\delta^{18}O$ crustal components, such as sedimentary material at the margin of the Kalahari Craton. Evolved Hf isotopic signatures (Hf(t)= -15–-6) and moderately elevated O isotopic data ($\delta^{18}O$ = 6–8 ‰) of the Cambrian granitic rocks from central DML indicate a significant incorporation of the pre-existing, old continental crust. In eastern DML, the suprachondritic Hf–Nd isotope signatures and moderate $\delta^{18}O$ values of the late Neoproterozoic granites (650–550 Ma) from the Sør Rondane Mountains support the view that they mainly originated from crust of the Tonian Oceanic Arc Super Terrane (TOAST). The post-540 Ma granites, however, have more evolved Hf and Nd isotopic compositions, suggesting an increasing involvement of older continental components during Cambrian magmatism. Nd isotopes of the Cambrian granitic rocks in DML display an increasingly more radiogenic composition towards the east with model ages ranging from late Archean to Mesoproterozoic times, which is in line with the isotopic trend of the Precambrian basement in this region. The late Neoproterozoic (>600 Ma) igneous rocks in central and eastern DML were emplaced in two independent subduction systems, at the periphery of the eastern Kalahari Craton and somewhere within the Mozambique Ocean respectively. The accretion and assembly of the TOAST to the eastern margin of the Kalahari Craton and their collision with surrounding continental blocks was followed by extensive post-collisional magmatism due to delamination tectonics and orogenic collapse in the Cambrian. The late Neoproterozoic–Cambrian rocks in DML thus record an orogenic cycle from subduction-accretion, continental collision to post-

collisional process during and after the assembly of Gondwana.

Key Words

Zircon U–Pb geochronology; Hf–O isotopes; Kalahari Craton; Gondwana; Continental collision; Crustal evolution

1. Introduction

Late Neoproterozoic – Cambrian times witnessed the transition from the break-up of Rodinia to the amalgamation of Gondwana (e.g., Hofmann et al., 1991; Li et al., 2008; Merdith et al., 2017). Blocks of East and West Gondwana were sutured along various late Neoproterozoic–early Paleozoic Brasiliano/Pan-African mobile belts including the major East African-Antarctic Orogen (EAAO), the latter of which extends from Saudi Arabia to Mozambique and into Dronning Maud Land (DML) in East Antarctica (Jacobs et al., 1998; Jacobs and Thomas, 2004). The EAAO records first accretionary and then continental collision tectonics during the closure of the Mozambique Ocean from 800 to 500 Ma (Stern, 1994; Meert and Van Der Voo, 1997; Jacobs et al., 2003a; Meert, 2003; Jacobs and Thomas, 2004; Collins and Pisarevsky, 2005; Bingen et al., 2009; Fritz et al., 2013; Mole et al., 2018; Jacobs et al., 2020). The southern part of the EAAO in DML records multiple episodes of magmatism and high-grade metamorphism from ca. 650 to 500 Ma (e.g., Jacobs et al., 2008a; Osanai et al., 2013; Elburg et al., 2016), which provides a key to understanding the amalgamation history of this region. Within Gondwana, western-central DML was attached to the eastern margin of the Kalahari Craton with the Grenville-age Maud Belt constituting the main basement (Groenewald et al., 1995; Jacobs et al., 2008b), while eastern DML is dominated by exotic 1000–900 Ma juvenile oceanic arcs (Tonian Oceanic Arc Super Terrane, TOAST, Jacobs et al., 2015) that were accreted onto the Kalahari Craton during the assembly of Gondwana (Fig. 1).

Igneous rocks generated during East African-Antarctic orogenesis provide important information on the crustal and tectonic evolution associated with subduction, accretion and collision processes. Particularly, the cessation of major orogenic events is marked by widespread post-collisional magmatism throughout the entire orogen (e.g., Küster and Harms, 1998; Stern, 2002; Veevers, 2007). In the southern part of the EAAO, voluminous Cambrian granites in Mozambique, Madagascar and East Antarctica (Jacobs et al., 2008a; Bingen et al., 2009; Goodenough et al., 2010; Archibald et al., 2019) are attributed to post-collisional delamination tectonics, followed by orogenic collapse (Jacobs et al., 2008a; Viola et al., 2008; Ueda et al., 2012). In western and central DML, Pan-African igneous rocks are dominated by 530–485 Ma post-collisional granites, syenites, charnockites and subordinate mafic rocks (Jacobs et al., 2008a). This magmatism is preceded by ca. 610–600 Ma anorthosite and charnockite magmatism in the easternmost part of central DML – at the eastern margin of the Kalahari Craton (Jacobs et al., 1998). Eastern DML in contrast, witnessed almost continuous granitic magmatism from 650 to 500 Ma (Elburg et al., 2016). Elucidating the formation and tectonic setting of late Neoproterozoic to Cambrian igneous rocks in DML is critical for the better understanding of the orogenic processes and evolution associated with the amalgamation of Gondwana in the southern part of the EAAO.

In this contribution, we present the first comprehensive U–Pb–Hf–O zircon data set and additional whole-rock Sm–Nd isotope and geochemistry data of late Neoproterozoic to Cambrian igneous rocks, along an E-W trending profile along the DML mountains. The new data provide new constraints on the age, origin and evolution of mostly granitic rocks across the eastern margin of Kalahari and into the TOAST. Based on compiled new and published data, we investigate the spatial and temporal variations in crustal composition and evolution along our profile, and relate this to the tectonic setting during closure of the Mozambique Ocean and the amalgamation of Gondwana in this key region of East Antarctica.

2. Geological background

The Jurassic rift margin escarpment of DML resulted in an approximately 1500 km long mountain range that offers a unique cross section through the southern part of the EAAO (Fig. 1), in an area that is otherwise largely ice-covered. Three major tectonic domains can be differentiated. In the west, the EAAO has reworked the easternmost part of the Kalahari Craton; the western orogenic front of the orogen is a major transcurrent shear zone, exposed in Heimefrontfjella. In the east, the EAAO has overprinted Indo-Antarctic crust, with a less well defined orogenic front. In between these two major blocks with African and Indo-Antarctic affinities lies the TOAST (Jacobs et al., 2015), interpreted as a remnant of the Mozambique Ocean, comparable to the Arabian-Nubian Shield. The contact of the easternmost Kalahari Craton with the TOAST is marked by the Forster Magnetic Anomaly that appears to be collinear with the South Orvin Shear Zone (Fig. 2). The Forster Magnetic Anomaly can be traced underneath the ice for a considerable distance to the south. The eastern boundary of the

TOAST is ill-defined and is probably somewhere close to the Yamato Mountains (Ruppel et al., 2018). To the south of the DML mountains, a cryptic craton, the Valkyrie Craton, may limit the southern extent of the TOAST (Jacobs et al., 2015; Golynsky et al., 2018) (Fig. 2). Our granitic samples provide a cross section from the easternmost Kalahari Craton into the TOAST, but do not cover the easternmost part of the orogen with an Indo-Antarctic affinity.

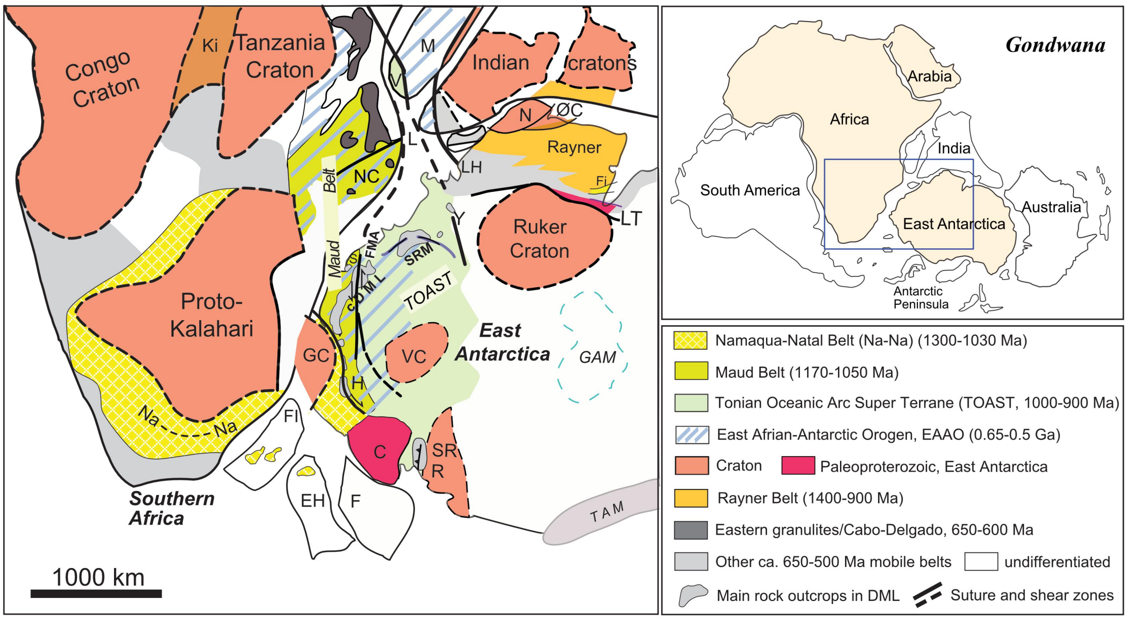

Fig. 1: Location of DML in East Antarctica (after Jacobs et al., 2017) and in Gondwana configuration during Paleo-Mesozoic times (after Gray et al., 2008). Abbreviations: C, Coats Land; cDML, central Dronning Maud Land; EH, Ellsworth-Haag; F, Filchner Block; FI, Falkland Islands; Fi, Fisher Terrane; FMA, Forster Magnetic Anomaly; GAM, Gamburtsev Mountains; GC, Grunehogna Craton; H, Heimefrontfjella; Ki, Kibaran; L, Lurio Belt; LH, Lützow-Holm Bay; LT, Lambert Terrane; M, Madagascar; N, Napier Complex; NC, Nampula Complex; Na–Na, Namaqua–Natal Belt; ØC, Øygarden Complex; R, Read Block; S, Schirmacher Oasis; SR, Shackleton Range; SRM, Sør Rondane Mountains; TAM, Transantarctic Mountains; V, Vohibori; VC, Valkyrie Craton; Y, Yamato Mountains.

2.1 Western-central DML

In western and central DML, the tectonically reworked margin of the easternmost Kalahari Craton is exposed. The region includes the Archean Grunehogna Craton, which was interpreted as part of the Kalahari Craton before the breakup of Gondwana (Groenewald et al., 1995; Jones et al., 2003; Marschall et al., 2010). It is surrounded by the eastern extension of the late Mesoproterozoic Natal

Belt to the south and the Maud Belt to the east (Fig. 2). The Maud Belt is largely exposed between H.U. Sverdrupfjella in the west and the Orvin-Wohlthat mountains in the east. It is interpreted as a major Grenville-age continental arc that formed at the periphery of Proto-Kalahari and Rodina (e.g., Marschall et al., 2013; Wang et al., 2020). The Mesoproterozoic basement of the Maud Belt in western and central DML is dominated by (meta-) volcanic and intrusive rocks formed between 1170 to 1090 Ma, which are intruded by 1090–1050 Ma A-type granite sheets and plutons accompanied by amphibolite to granulite facies metamorphism (Jacobs et al., 2003a, 2003b; Paulsson and Austrheim, 2003; Board et al., 2005; Bisnath et al., 2006; Grantham et al., 2011). Hf and Nd isotopes of the Grenville-age basement exhibit an obvious variation from the west to east, with H.U. Sverdrupfjella showing significantly negative epsilon values and Archean model ages, while Gjelsvikfjeik and the Orvin-Wohlthat Mountains have Paleoproterozoic to Mesoproterozoic model ages. This indicates the large involvement of older cratonic crust in the west and successively more juvenile rocks towards the east (Wang et al., 2020).

After a period of tectonic quiescence, renewed continental arc magmatism commenced at ca. 780 Ma, as is evident from the Schirmacher Oasis (Jacobs et al., 2020). The Maud Belt has thereafter been tectonically reworked at amphibolite- to granulite-facies grade during East African-Antarctic orogenesis between ca. 650 and 500 Ma (Moyes et al., 1993a; Groenewald et al., 1995; Moyes and Groenewald, 1996; Board et al., 2005; Pant et al., 2013; Pauly et al., 2016). Protracted late Neoproterozoic/early Paleozoic tectono-metamorphism is recorded in metamorphic zircon rims at 600 Ma, 580–550 Ma and 530–515 Ma (e.g., Jacobs et al., 1998; Baba et al., 2015; Wang et al., 2020). The late Neoproterozoic (650 – 600 Ma) UHT metamorphism (peak conditions: 950–1050^{o} C, 0.9–1.0 GPa, Baba et al., 2006, 2010) and syn-tectonic magmatism may relate to a period of back-arc extension of the eastern Kalahari Craton (Baba et al., 2010; Jacobs et al., 2020). During this stage, anorthosite and charnockite magmatism is recorded in the easternmost part of central DML (Grubergebirge). Subsequently, at ca. 580–550 Ma, western-central DML experienced crustal thickening with peak metamorphism reaching (eclogite)granulite-facies (>900^{o} C, 1.5 GPa) (Pauly et al., 2016; Palmeri et al., 2018) followed by isothermal decompression, constituting a clockwise P-T path (Colombo and Talarico, 2004; Bisnath and Frimmel, 2005; Baba et al., 2008; Elvevold and Engvik, 2013; Pauly et al., 2016; Palmeri et al., 2018; Elvevold et al. 2020). This was interpreted as a result of continental collision between the Kalahari Craton and other crustal terranes. Accompanying high-grade metamorphism, the Mesoproterozoic basement has also experienced migmatisation, but major synchronous granitic plutons have not been recognized thus far. In Cambrian times, orogenic collapse and extensional tectonics led to the emplacement of large volumes of late-tectonic igneous rocks at ca. 530–485 Ma, including charnockites, syenites, granites and gabbros (Jacobs et al., 1998, 2003a, b, 2008).

Thus, late Neoproterozoic–Cambrian igneous rocks in western-central DML were mainly emplaced in two periods at ca. 650–600 Ma and at ca. 530–485 Ma. The continental collision stage is characterized by migmatites and granulites and lacks significant volumes of syn-tectonic plutonic rocks, whereas the Cambrian orogenic collapse stage provides the by far largest volumes of granitoids in this part of the EAAO.

2.2 Eastern DML

A recent aerogeophysical survey over eastern DML has revealed an extensive tectonic block (SE DML province, Fig. 2), characterised by low amplitude, elongate, NW-SE trending magnetic anomalies (Mieth et al., 2014). It is dominated by a distinct suite of gabbro-tonalite-trondhjemite-granodiorites (GTTG) dated at ca. 1000–900 Ma (e.g., Jacobs et al., 2015), which are tectonically interleaved with volcano-sedimentary rocks. The GTTGs are interpreted as juvenile oceanic arc crust, based on their geochemistry, juvenile Sm–Nd and zircon Hf-signature, as well as the lack of older inheritance (Kamei et al., 2013; Elburg et al., 2015; Jacobs et al., 2015). The volcano-sedimentary rocks include marbles, calcsilicates, garnet-sillimanite gneisses, graphite schists and heterogeneous quartzo-feldspathic gneisses, interpreted as a meta-volcano-sedimentary sequence of the Mozambique Ocean (Elburg et al. 2015; Jacobs et al., 2015; Kamei et al., 2013). Detrital zircons of the metasedimentary rocks show very limited pre-Tonian provenance (Kitano et al., 2016), in line with the juvenile characteristic of this region. The GTTGs and the associated volcano-sedimentary rocks together form the TOAST (Jacobs et al., 2015). The formation of the TOAST is probably related to the amalgamation of a number of oceanic island arcs during late Neoproterozoic times (Baba et al., 2013; Ruppel et al., 2020). The latest geophysical investigations show that the TOAST may extend into the Belgica and Yamato mountains towards the east, and thus represents a significant region with a size of over 500,000 km^2, sandwiched between the Kalahari Craton in the west and an Indo-Antarctic craton in the east (Ruppel et al., 2018).

The tectonically reworked TOAST is exposed in the Sør Rondane Mountains (SRM), where it shows various degrees of tectono-metamorphism, dated at ca. 650–500 Ma, and ranging from granulite facies to greenschist facies (e.g., Osanai et al., 2013). The SRM has been divided into two terranes with different late Neoproterozoic to Cambrian metamorphic histories, the Northeast (NE) and the Southwest (SW) Terrane (Osanai et al., 2013), with the boundary defined as the 'Main Tectonic Boundary' (Fig. 2). The SW Terrane is characterized by a counterclockwise P–T path with isothermal compression at the initial stage of metamorphism and retrograde isobaric cooling, while the NE Terrane yield a clockwise P–T path with decompression and cooling processes (Adachi et al., 2013; Baba et al., 2013; Osanai et al., 2013). The peak granulite facies metamorphism was dated at 650–600 Ma and interpreted as a result of the overthrusting of the NE Terrane over the SW Terrane (Adachi et al., 2013; Osanai et al., 2013). The subsequent 590–530 Ma thermal events were attributed to continental collision between the Kalahari Craton and Indo-Antarctica (Shiraishi et al, 2008; Boger, 2011; Osanai et al., 2013). At least four phases of late Neoproterozoic–Cambrian magmatic activities have been identified in the SRM. The oldest Ediacaran magmatic activity is represented by the granitic magmatism in the Dufek area and the reported ages range from ca. 640 Ma to 620 Ma (Li et al., 2006; Elburg et al., 2016), followed by a suite of 570–550 Ma garnet-leucogneisses, granite sheets and minette dykes (Shiraishi et al., 2008; Owada et al., 2013; Elburg et al., 2016). The ca. 530 Ma granites are distributed across the SW Terrane from west to east (Elburg et al., 2016), while the latest magmatism occurred at 510–500 Ma, producing mafic and granitic intrusions (Owada et al., 2008; Elburg et al., 2016).

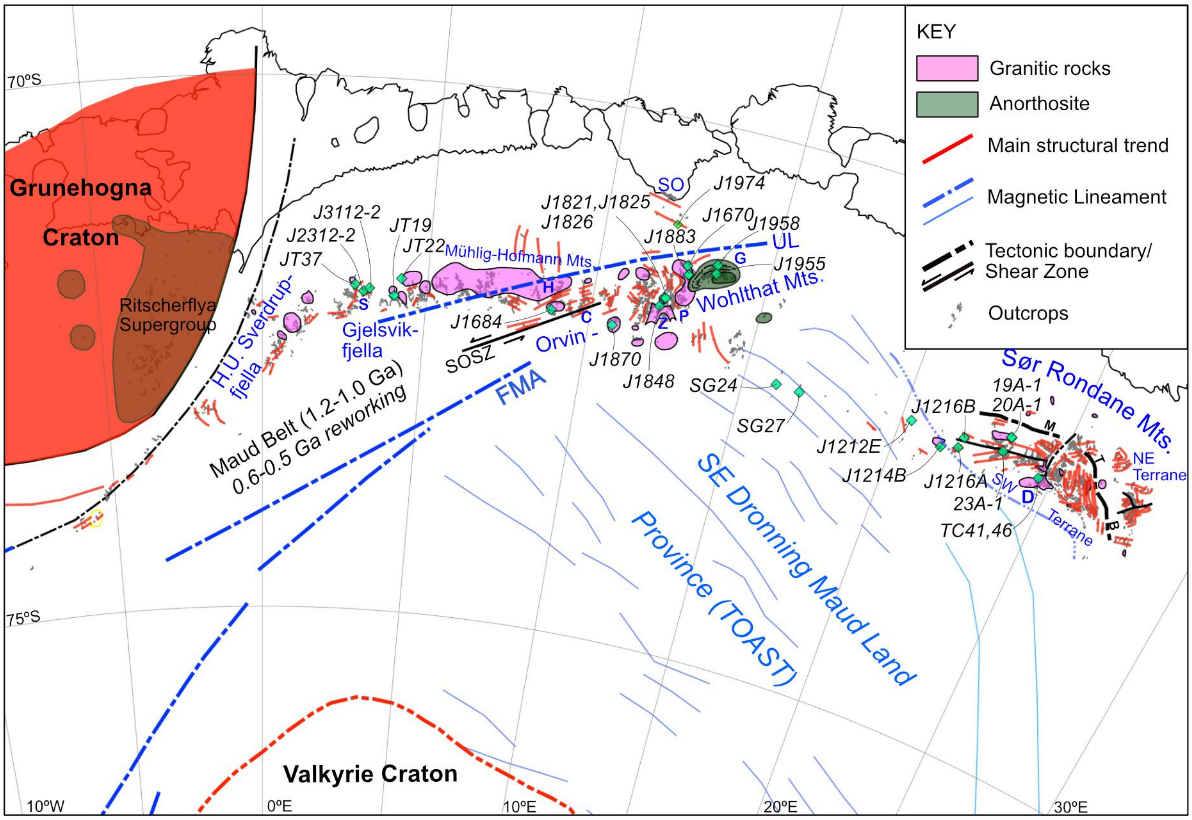

Fig. 2: Geological overview map of the study area and sample localities in central and eastern DML. Abbreviations: C, Conrad mountain; D, mount Dufek; FMA, Forster Magnetic Anomaly; G, Grubergebirge; H, Holtedahlfjella; MTB, Main Tectonic Boundary; P, Petermannketten; S, mount Stabben; SO, Schirmacher Oasis; SOSZ, South Orvin Shear Zone; TOAST, Tonian Oceanic Arc Super Terrane; UL, Ulvetanna Lineament; Z, mount Zwiesel.

3. Samples and analytical methods

The samples in this study were collected during four expeditions between 1995 and 2018. The core of this study consists of 27 granitic and gabbro samples that were collected from Gjelsvikfjella in the west, across the Orvin-Wohlthat Mountains (central DML) to the SRM (eastern DML) in the east (Fig. 2, Table 1). The combined U–Pb–Hf–O zircon results constitute a W-E oriented isotopic profile across the reworked eastern margin of the Kalahari Craton and a significant part of the tectono-thermally reworked part of the TOAST. Our study utilized in part samples from previous studies, for which U–Pb zircon data were already available (Jacobs et al., 1998, 2003a, 2015, Suliman, 2011). All Hf–O zircon data of this study are new.

Moreover, whole-rock Sm–Nd isotope analyses have been conducted on 34 granitic samples from central and eastern DML. They include three dated samples from the SRM, eastern DML, whilst the other 31 granitic samples (samples of Roland, 2004) from the Orvin-Wohlthat Mountains of central DML are undated. As the late voluminous granitic rocks in central DML are all Cambrian in age (Jacobs et al., 2008a and dating results in this study), it is inferred that the latter samples have igneous crystallization ages between ca. 510–485 Ma.

Detailed analytical methods are provided in Supplementary File A.

3.1 Zircon U–Pb dating and Hf–O isotopes

Optical (reflected and transmitted light) and cathodoluminescence (CL) images were taken on zircons prior to U–Pb analyses to reveal the internal textures and to guide the selection of analysis spots. U–Pb, Lu–Hf and O isotopic analyses were mostly performed on the same spot or from the same growth domain.

Zircon U–Pb dating on most samples from central DML was carried out using the Sensitive High Resolution Ion Microprobe (SHRIMP) at the IBERSIMS Laboratory, University of Granada, Spain. Three samples were dated by LA-ICP-MS at the University of Bergen. Four samples from eastern DML were analysed using a CAMECA IMS-1280 instrument at the NordSIM facility, Stockholm Museum of Natural History (Sweden). For most samples, we report ^{204}Pb-corrected ages, while ^{208}Pb-corrected ages are used for samples with low Th and U concentrations. Weighted mean ages and group concordia ages are calculated with Isoplot (Version 4.15; Ludwig, 2011). All errors are reported at the 2σ-level. Oxygen isotope ratios of zircon grains were measured at the NordSIM and IBERSIMS laboratories. Prior to O-ion microprobe analysis, the U–Pb analysis spots were removed from the zircons by polishing, followed by recoating with ~30 nm gold. The values of average δ^{18}O values are reported as mean ± 2 standard deviation (S.D.).

Lu–Hf isotopes were measured at the University of Johannesburg, using an ASI 265 Resonetics 193 nm Excimer laser ablation system coupled to a Nu Plasma II multi-collector ICPMS. For calculation of the epsilon Hf, the chondritic uniform reservoir (CHUR) was used as recommended by Bouvier et al. (2008) (^{176}Lu/^{177}Hf and ^{176}Hf/^{177}Hf of 0.0336 and 0.282785, respectively), and a decay constant of 1.867×10^{-11} (Scherer et al., 2001; Söderlund et al., 2004). The calculation of model ages is based on the depleted mantle source values of Griffin et al. (2000) with present-day $^{176}Hf/^{177}Hf$ = 0.28325 and $^{176}Lu/^{177}Hf$ = 0.0384. Initial $^{176}Hf/^{177}Hf$ and εHf values for all analysed zircon domains were calculated using the respective interpreted crystallization age of each sample. The values of average εHf (t) and $^{176}Hf/^{177}Hf_{(i)}$ for each sample are reported as mean ± 2 S.D.

3.2 Whole-rock Sm–Nd isotope and geochemistry

Sm–Nd isotope data were acquired at the University of Bergen, Norway and the University of Tübingen, Germany. Calculation of the Sm–Nd model parameter εNd is based on $^{143}Nd/^{144}Nd$ = 0.512638 and $^{147}Sm/^{144}Nd$ = 0.1967 for a CHUR reference ('chondritic uniform reservoir', Jacobsen and Wasserburg, 1980). Single-stage depleted-mantle model ages (T_{DM}) were calculated assuming $^{143}Nd/^{144}Nd$ = 0.51315 and $^{147}Sm/^{144}Nd$ = 0.2137 for the present-day depleted-mantle reservoir and a linear Sm/Nd evolution trough time. Whole-rock element analyses were conducted at the University of Johannesburg, South Africa and the University of Tübingen, Germany.

4. Results

Detailed zircon U–Pb dating and Hf–O isotopic data are provided in Supplementary File B, and whole-rock geochemical and Sm–Nd isotopic data are presented in Supplementary File C. A summary of key sample information and U–Pb–Hf–O results in this study are summarized in Table 1.

4.1 Zircon U–Pb geochronology of samples from central DML

4.1.1 Late Neoproterozoic (650 – 630 Ma) samples

Two samples from the Petermannketten, including one charnockitic gneiss (J1883) and one garnet-bearing granitic gneiss (J1848), have late Neoproterozoic igneous crystallization ages (Fig. 3). Most zircons from these two samples are characterized by core-(mantle)-rim structures (Fig. 3b, d). The cores display clear oscillatory zoning and high Th/U ratios between 0.3 and 0.5, and thus are interpreted as igneous zircons. In contrast, the rims are invariably CL-dark, structureless and have low Th/U ratios (<0.1), consistent with the characteristics of metamorphic zircons. As for sample J1883, twenty-nine analyses were conducted on 27 grains, including 23 oscillatory-zoned domains and 6 rims. Eight core analyses define a concordia age of 645 ± 6 Ma (MSWD = 1.18), which is interpreted as the igneous crystallization age of igneous protolith; many other core analyses are discordant due to Pb-loss. Five rim analyses define a common concordia age of 592 ± 8 Ma (MSWD = 0.94), which is interpreted as the time of metamorphic overprint (Fig. 3a). Similarly, the igneous crystallization age of sample J1848 is determined by 5 core analyses, which give a well-constrained concordia age of 628 ± 7 Ma (MSWD = 1.14) (Fig. 3c). Eighteen rims and three cores, which show no zoning but with similar ages than the rims, yield a common concordia age of 562 ± 3 Ma (MSWD = 1.3), which is interpreted as the timing of high-grade metamorphic overprint. In addition, three core analyses are (nearly) concordant at ca. 680 Ma, probably representing zircon inheritance.

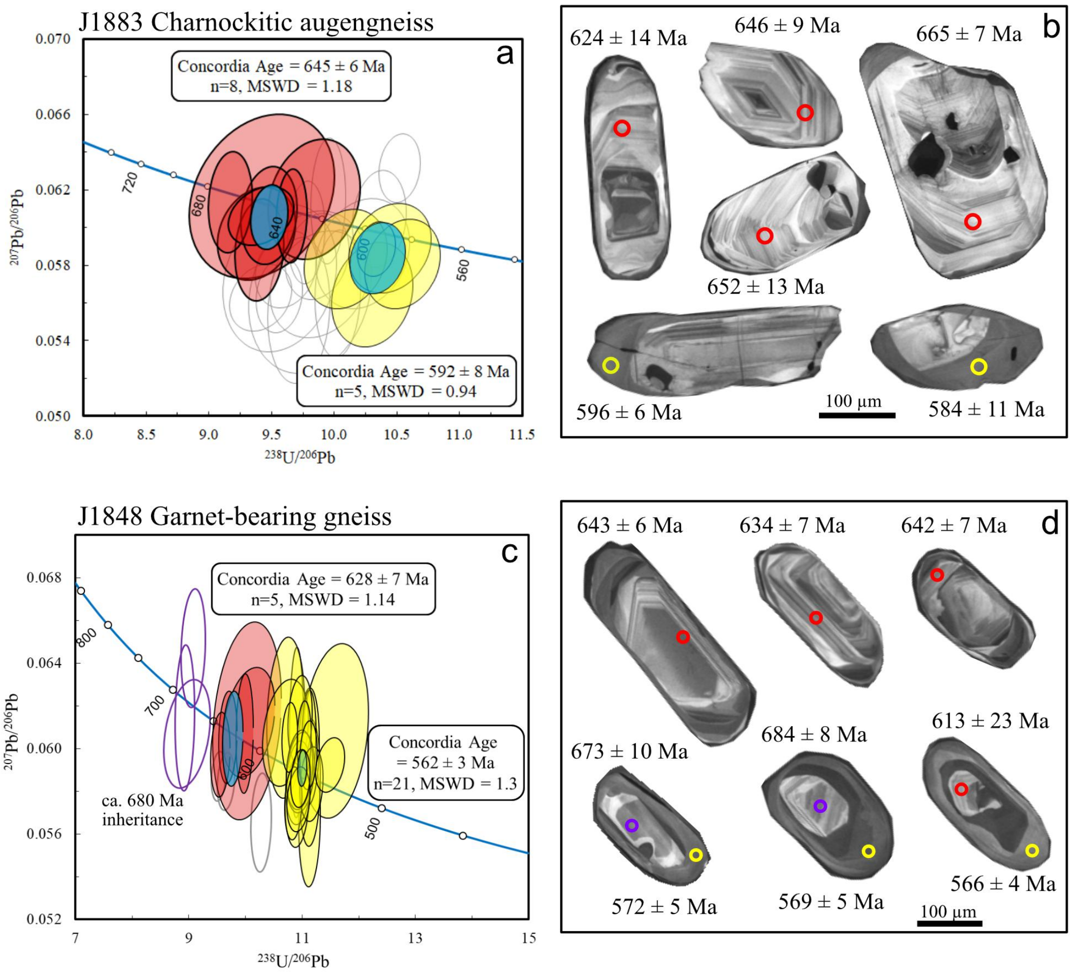

Fig. 3: U–Pb Tera-Wasserburg diagram and CL images of two late Neoproterozoic granitic samples from central DML. In the Tera-Wasserburg diagrams, red and yellow filled ellipses indicate concordant igneous and metamorphic zircons respectively with concordia ellipse in blue. The grey ellipses indicate discordant zircon analyses and purple ones are inherited zircons; CL images show core (red) - rim (yellow) structures, representing igeous crystallization and metamorphic domains respectively.

4.1.2 Cambrian (530–485 Ma) samples

This sample group includes two gabbros and five granitic samples from Gjelsvikfjella and the Orvin-Wohlthat Mountains (Table 1). Most zircon grains of the individual samples have typical euhedral to subhedral shapes with sizes between ca. 150 and 450 µm, and their internal structure shows mostly simple oscillatory zoning, interpreted as magmatic growth zoning. Gabbro sample JT 37 is one of the westernmost samples (mount Stabben) of this study. Eight concordant analyses provide a concordia age of 483 ± 4 Ma (MSWD = 0.79) (Fig. 4a), which is slightly younger than the associated Stabben syenite (500 ± 8 Ma, Paulsson and Austrheim, 2003). Two granitic samples from Gjelsvikfjella yield concordia ages of 500 ± 3 Ma (n=14, MSWD = 0.81) (charnockite, JT19) and 499 ± 4 Ma (n=9, MSWD = 1.07) (granite JT22) respectively (Fig. 4b, c). These ages indicate a pulse of Cambrian gabbroic and granitic magmatism between 500–485 Ma in Gjelsvikfjella. Further east, granite sample J1684 has an igneous crystallization age of 486 ± 7 Ma (n=16, MSWD = 0.83) (Fig. 4d). Further east at mount Zwiesel, the igneous crystallization ages of three gabbroic and granitic samples range from ca. 525 Ma to ca. 495 Ma (Fig. 4e–g). The age of the gabbro sample (J1826, 524 ± 2 Ma, n=17, MSWD = 1.3) is within error of the published ages in this region (521 ± 6 and 527 ± 5 Ma, Jacobs et al., 2003), defining the oldest late-tectonic age in this study. Two granitic samples from this region have younger igneous crystallization ages of 514 ± 5 Ma (charnockite J1821, n=39, MSWD=0.50) and 494 ± 6 Ma (syenite J1825, n=15, MSWD=0.56). Precambrian inheritance is revealed by a few samples, including Grenville-age (1090–1060 Ma) and late Neoproterozoic (610–600 Ma) ages.

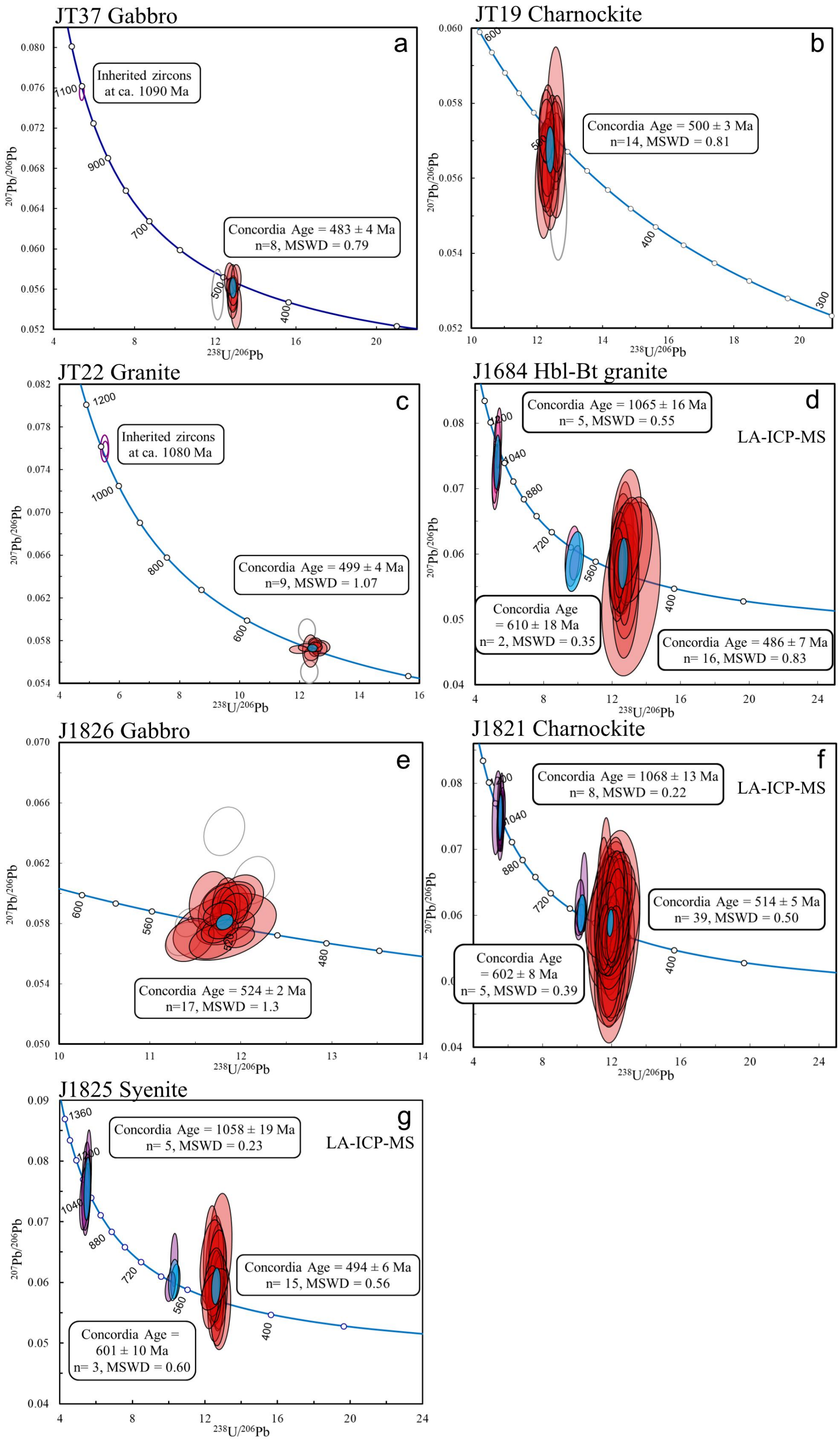

Fig. 4: U–Pb Tera-Wasserburg diagram of the Cambrian samples from central DML. The colour coding is the same as in Fig. 3. The dating data of three samples analysed by LA-ICP-MS are from Suliman (2011). CL images for each sample can be found in Supplementary File B.

4.2 Zircon U–Pb geochronology of granites from eastern DML

Five new granite samples were dated from the SW terrane of the SRM, including two granites from mount Dufek and three from adjacent regions to the west. In CL, the zircon grains of two Dufek granites (TC-46, TC-41) are dominated by oscillatory-zoned cores surrounded by dark and structureless rims. In sample TC-46, all analyses were conducted on cores, which define two concordia age groups at 612 ± 2 Ma (n=7, MSWD = 0.37) and 606 ± 1 Ma (n=6, MSWD = 1.4) respectively. This may indicate a progressive zircon crystallization over a period of several millions of years. The weighted mean age (607 ± 2 Ma, MSWD = 3.4) agrees within error with the second concordia age group (Fig. 5a). Therefore, the latter concordia age is used here to represent the closest approximation of the crystallization age of the Dufek granite. The zircon core and rim analyses of sample TC-41 show a significant scatter from ca. 600 to 550 Ma. Seven oldest concordant analyses, including 5 cores and 2 rims, give a concordia age of 588 ± 4 Ma (MSWD = 1.5) (Fig. 5b), which is interpreted as the crystallization age of this sample. Five concordant rims define a concordia age of 579 ± 4 Ma (MSWD = 1.2). These rim analyses generally have higher U (1800–4100 ppm) and lower Th/U (ca. 0.1) than the core analyses (U<350 ppm, Th/U=0.4–0.7), and they are thus interpreted as metamorphic rims; the age probably represents the timing of a later thermal event postdating granite crystallisation. The U–Pb isotopic system of some cores with high U (500–5000 ppm) and lower Th/U (0.2), may have been reset during a second subsequent thermal event, with a young concordant age group providing a concordia age of 547 ± 2 Ma (n=5, MSWD = 0.95).

Zircon grains from the remaining three granite samples (23A-1, 20-1, 19A-1) generally have typical igneous zircons with oscillatory zoning. Their U–Pb data define their igneous crystallisation ages at 555 ± 4 Ma (n=8, MSWD = 1.3), 524 ± 3 Ma (n=9, MSWD = 0.99) and 521 ± 2 Ma (n=13, MSWD = 0.70) (Fig. 5c-e) respectively. Ediacaran inheritance of ca. 620 Ma is present in one of the samples (Fig. 5c).

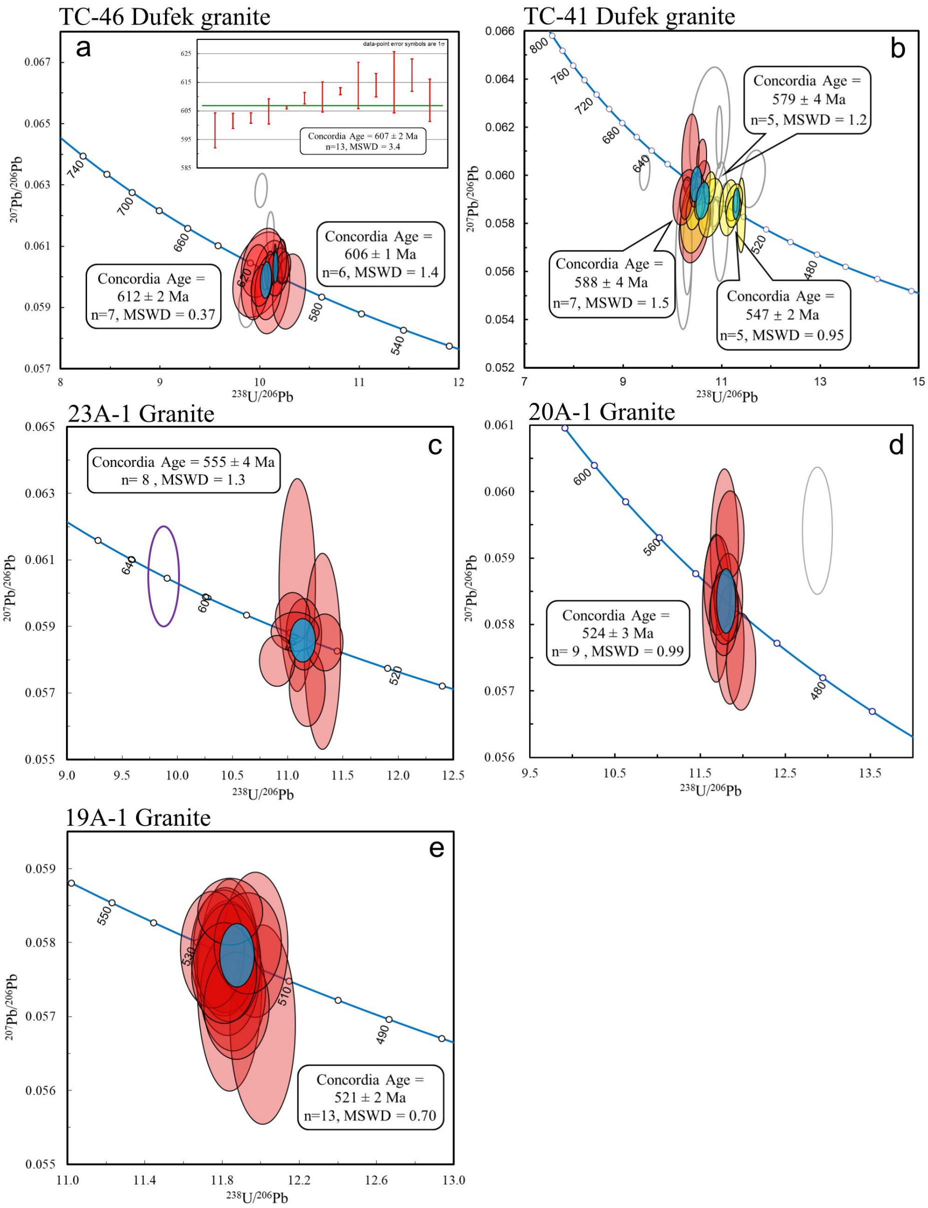

Fig. 5: U–Pb Tera-Wasserburg diagram of the granite samples from eastern DML. The colour coding is the same as in Fig. 3. CL images for each sample can be found in Supplementary File B.

4.3 Major and trace elements

The geochemical characteristics are illustrated in Fig. 6. The granitic rocks from central DML have overall moderate to high silica (SiO_2=60–71wt.%), mostly plotting in the quartz monzonite and granite fields on the TAS diagram (Fig. 6a). They have alkali contents (Na_2O+K_2O) of 6.0–10.9 wt.%, and the modified alkali–lime index of Frost et al. (2001), MALI, varies from 1.05 to 9.06; the samples therefore plot in alkaline and alkali-calcic fields (Fig. 6b). In the K_2O versus SiO_2 diagram, most samples plot in the shoshonitic field, whereas a few display high-K affinities (Fig. 6c). They are generally metaluminous to slightly peraluminous with molar $Al_2O_3/(CaO+Na_2O+K_2O)$ ratios of 0.83–1.09 (Fig. 6e). The Fe-index (FeO*/(FeO*+MgO)) ranges from 0.75 to 0.85, which demonstrates their ferroan character (Fig. 6d). In the A-type granite discrimination diagram, both quartz monzonite and granite samples show high $10^4 * Ga/Al$ (>2.6), pointing to A-type granites (Whalen et al., 1987) (Fig. 6f). On the primitive mantle-normalized spidergram, all samples are characterized by positive anomalies of Rb, Th, U and LREE (La, Ce, Nd, Sm) as well as Pb, but negative anomalies in Sr, Nb, P and Ti (Fig. 6g). Most samples have a zircon-saturation temperature over 800–850°C (Fig. 6h).

The granitic samples from SRM are overall similar to the central DML samples in major element composition, and most of them have a geochemical affinity to metaluminous, alkaline to alkali-calcic, ferroan A-type granite; however, a significant subgroup displays a magnesian character and contains lower alkali contents. Generally, the Cambrian samples (540–500 Ma) have a higher SiO_2 and lower alkali concentration than the older 590–550 samples. The trace element concentration and patterns are similar with the central DML samples. Their zircon-saturation temperatures are commonly lower than 850°C (Fig. 6h).

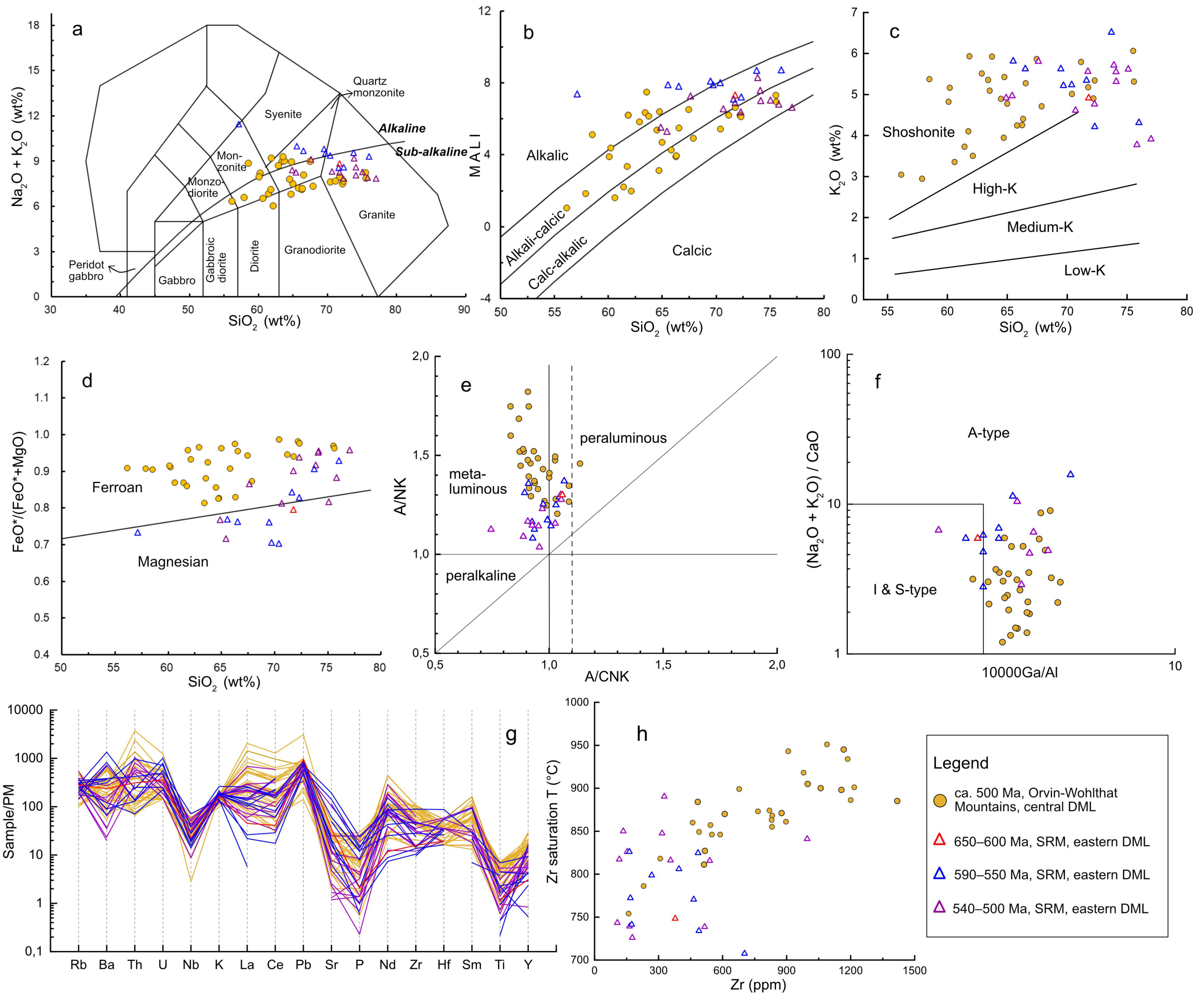

Fig. 6: Geochemical characterisation of late-Neoproterozoic to Cambrian granitic rocks from DML. (a) Discrimination diagram from Middlemost (1994), grey dividing line between alkaline and subalkaline series is from Irvine and Baragar (1971); (b) MALI (modified alkaline lime index, Na_2O+K_2O-CaO, wt%) versus SiO_2 diagram of Frost et al. (2001) represents the range varying from alkalic to moderate alkali-calcic to calc-alkalic field of studied samples; (c) SiO_2-K_2O diagram (after Gill, 1981); (d) Fe-index vs. wt% SiO_2 (Frost, 2001), showing that most samples plot in the field of ferroan granite; (e) Aluminum saturation index (ASI) plot of Maniar and Piccoli (1989), (Al/Na + K) and (Al/Ca + Na + K) are defined as molecular ratios; (f) 10^4*Ga/Al vs $(Na_2O+K_2O)/CaO$ diagram after Whalen et al. (1987) to identify A-type granites from S-or I-type; (g) Primary mantle (PM) normalized trace element spider patterns; (h) Zr vs. Zr saturation temperature diagram, the equation follows Boehnke et al. (2013).

4.4 Zircon Hf–O isotopic composition

Zircon O and Hf isotopic results are illustrated in Fig. 7 and Fig. 8 respectively. The 645–600 Ma charnockites (J1883 and J1886) and anorthosite samples (J1955 and J1958) from the eastern Orvin-

Wohlthat Mountains have homogeneous zircon Hf–O isotopic compositions. They are characterized by enriched heavy O isotopic composition with $\delta^{18}O$ values between 8‰ and 9‰ (Fig. 7a); εHf(t) values are mostly neutral with averages between +0.7 and +1.4. Zircons grains from a garnet-gneiss sample dated at 636 Ma (J1848) have a similar Hf–O isotopic signature, with εHf(t) values yielding an average of +1.0 ± 1.4 and $\delta^{18}O$ value of 8 – 9‰.

The 530 – 485 Ma mafic and granitic samples from the western part of central DML in Gjelsvikfjella (JT19, JT22, 3112-2, 2312-2, JT37) have an average of mantle-like and mildly higher $\delta^{18}O$ values of 5.7–6.5‰ (Fig. 7a). One lamprophyre dyke (2312-2) has unradiogenic εHf(t) values of -4.1–-0.9, while the other four samples have significantly evolved Hf isotopic compositions with average εHf(t) of -12–-7. Similarly, the ca. 500 Ma granitic rocks (J1870, J1670) from the Orvin-Wohlthat Mountains display more evolved Hf isotopic composition with εHf(t) values of -8.8 – -5.6 than the ca. 525 Ma gabbro (J1826, εHf(t) = -3.7 – -1.7) (Fig. 8a), while their $\delta^{18}O$ values are generally moderately elevated at 7.0–8.0 ‰.

One amphibolite gneiss (J1212E, ca. 925 Ma) of the TOAST and nine granites (610 – 500 Ma) have been analysed for their zircon Hf and O isotopic compositions. The older TOAST sample has moderately elevated $\delta^{18}O$ values of 6 – 7‰ and juvenile Hf isotopic compositions (εHf(t) values at ca. +5.5). Oxygen isotopic compositions of the granites appear to be unrelated to the igneous ages, but largely controlled by their location. Seven granite samples from the SRM mostly have moderate $\delta^{18}O$ values of 6 – 7‰, but two granites from SE DML have higher $\delta^{18}O$ values between 7 and 9‰ (Fig. 7b). Their Hf isotopes exhibit an obvious variation from Ediacaran to Cambrian times, with the older pre-540 Ma granites showing positive εHf(t) values while the Cambrian granites having negative εHf(t) values of -5 – -1 (Fig. 8b).

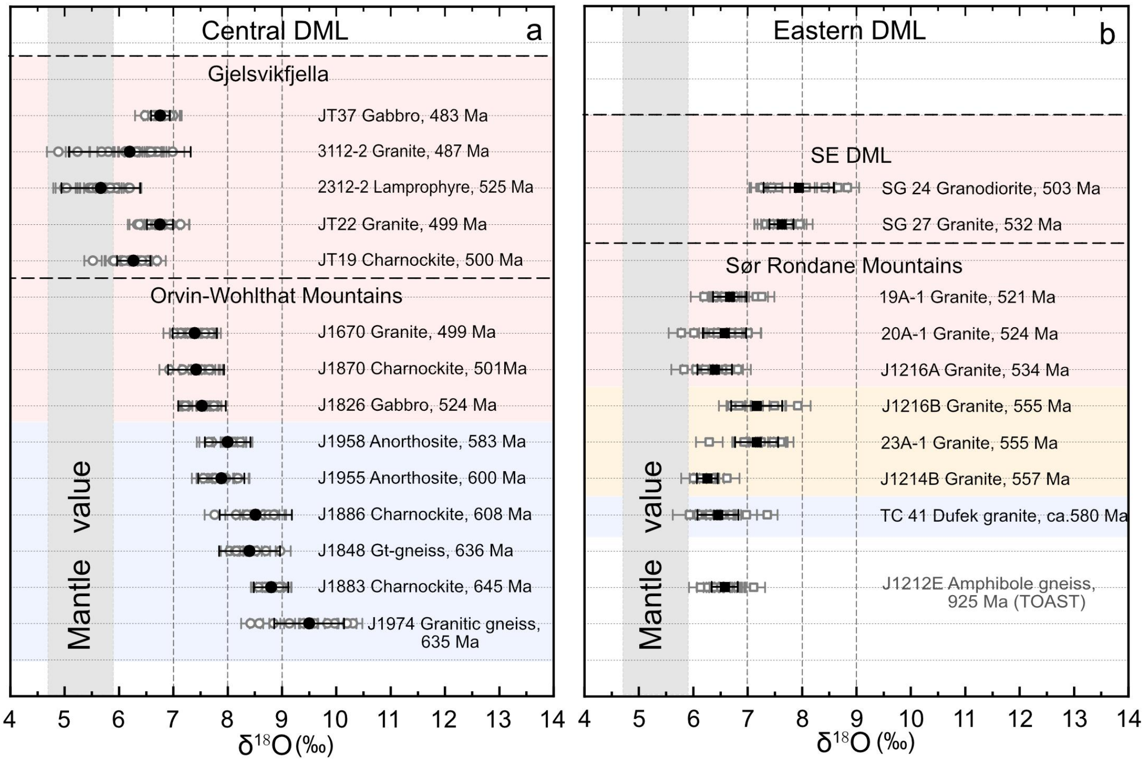

Fig. 7: Zircon oxygen isotope values of 650–485 Ma samples and one ca. 925 Ma (TOAST) sample from central and eastern DML. The grey symbols show individual spot values, whilst the black ones show average values for each sample. Mantle values are 5.3 ± 0.6‰, 2σ (Valley et al., 1998). Light blue, yellow and red colours show >580 Ma, 570–550 Ma and 530–485 Ma samples respectively.

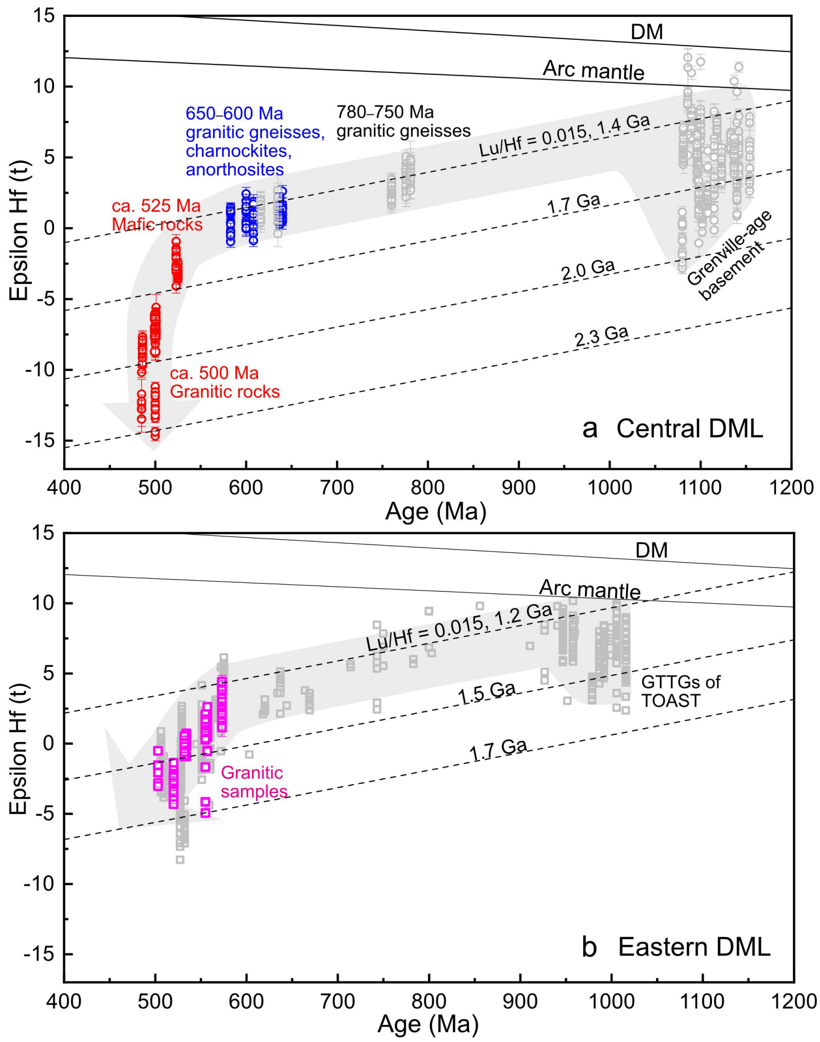

Fig. 8: Time versus εHf (t) plot of samples from central DML (a) and eastern DML (b). The evolution curve of arc mantle is from Dhuime et al. (2011). The Cambrian mafic and granitic rocks from central DML have an evolved Hf isotopic composition. Moreover, εHf (t) values of granitic rocks are significantly lower than mafic rocks. The granites from eastern DML are overall more radiogenic than those from central DML, but show an evolution that negatively deviates from the evolution array of 1.2 Ga crust. The light grey fields show the isotopic trends from the Meso-Neoproterozoic to the Cambrian. The grey samples in (a) show the Hf isotopes of Grenville-age basement in central DML (Wang et al., 2020) and 780–630 Ma gneisses from the Schirmacher Oasis (Jacobs et al., 2020); the grey samples in (b) show the Hf isotopes of 1000–900 Ma TOAST rocks, 650–500 Ma SRM granites as well as the scattered inherited zircons therein (Elburg et al., 2015, 2016).

4.5 Whole-rock Sm–Nd isotopic composition

Sm–Nd isotopic data of the Cambrian granitic samples from central DML are presented in Table 3, Supplementary File C and are illustrated in Fig. 11b. As ca. 500 Ma marks the most voluminous granitic magmatism in central DML (compiled data in Table 4 of Supplementary File B), this age is used in this study for the calculation of initial Nd isotopic values. Overall, initial εNd values are strongly to moderately unradiogenic with values ranging from -14 to -3, and model ages (T_{DM}) show a wide range from Paleoproterozoic to Mesoproterozoic times (2.1 – 1.4 Ga). In contrast, the granites from SRM have slightly negative to positive εNd(t) values and younger model ages at ca. 1.2 Ga (Fig. 11b).

5. Discussion

5.1 Late Neoproterozoic to Cambrian geochronological framework of DML

5.1.1 Central DML

The new U–Pb zircon data of this study, together with compiled published geochronological results, provide a refined temporal framework for the late Neoproterozoic to Cambrian magmatic activity in DML. The magmatic and metamorphic ages have been compiled and plotted in Fig. 9, in order to show and compare the distribution of different age groups. Two new igneous crystallization ages of ca. 645 and 630 Ma are obtained from one charnockite augengneiss (J1883) and one garnet gneiss (J1848), which represent the oldest known Neoproterozoic magmatism in central DML (except the Schirmacher Oasis). Subsequently, 610–600 Ma anorthosite and charnockite were emplaced in the Grubergebirge, the easternmost exposures of central DML (Jacobs et al., 1998). The 650–600 Ma charnockite and anorthosite magmatism is accompanied by high-grade metamorphism up to (U)HT-HP granulite facies (Baba et al., 2010). The emplacement of Cambrian magmatic rocks in central DML post-dates 590–560 Ma high-grade metamorphism and migmatization (Jacobs et al., 1998; Pauly et al., 2016), which occurred across almost the entire region. The reported magmatic ages in this period are rare, possibly in part due to sampling bias, and lack of availability of dated migmatitic rocks from areas such as Gjelsvikfjella. Cambrian magmatism (530–485 Ma) produced a series of granitic rocks, gabbros and mafic dykes across central and western DML. The granitic rocks are exposed throughout central DML, while the gabbro occurrences are relatively small, with the largest massif located at mount Zwiesel, eastern part of the Orvin-Wohlthat Mountains. The oldest post-collisional rocks so far dated is a meta-diorite from central Conrad (530 Ma, Jacobs et al., 2003a), almost synchronous with the gabbro intrusions at mount Zwiesel, which were dated at ca. 525 Ma (this study; Jacobs et al., 2003b). Subsequently, voluminous granitic magmatism, which generated charnockites (J1821, 514 Ma), syenite (512 Ma), anorthosite (506 Ma) (Mikhalsky et al., 1997), granites and minor gabbros (500–485 Ma, this study and Jacobs et al., 2008a), accompanied by high-grade metamorphism and anataxis, formed at 515–485 Ma. These ages thus define an overall continuous period of post-collisional magmatism in central DML from 530 to 485 Ma, accompanied by widespread metamorphism that affected the entire region of western-central DML as very commonly recorded by zircon rims and felsic leucosomes in migmatites.

The Cambrian granitic samples have usually very minor zircon inheritance. Inheritance-poor granitic magmas are usually generated under large heat input into the crust (Miller et al., 2003), which is consistent with the high zircon saturation temperature observed in the central DML samples (Fig. 6h). However, the limited Precambrian inheritance in 515–485 Ma samples in this study appears to differ in the western and eastern parts of central DML. Only older, i.e. ca. 1090–1080 Ma, inherited ages were recorded by the granite and gabbro samples (JT22 and JT37) in Gjelsvikfjella, whereas the inherited zircons from the Orvin-Wohlthat Mountains (J1821, J1825 and J1684) show both Grenville-age (1070–1060 Ma) and late Neoproterozoic (610–600 Ma) ages. The 615–600 Ma crust appears to have comprised an important composition of continental crust in the eastern part of central DML and contributed to the formation of Cambrian magmas. The ages of Cambrian magmatic activities also exhibit a spatial variation from west to east. The reported ages in Gjelsvikfjella are mostly around or younger than 500 Ma (Paulsson and Austrheim, 2003; Jacobs et al., 2003; Bisnath et al., 2006), except one older age at ca. 523 Ma obtained from a lamprophyre dyke (Jacobs et al., 2003a). Similarly, in H.U. Sverdrupfjella, western DML, the granite intrusions were dated at ca. 490–470 Ma (Grantham et al., 2011; Pauly et al., 2016) and older ages have not been reported so far. In contrast, the earlier-stage (530–515 Ma) mafic and granitic magmatism appears to be restricted to the east of the Ulvetanna Lineament.

5.1.2 Eastern DML

The granitic magmatism in the SRM lasted from Neoproterozoic to Cambrian times over a period of approximately 150 Myr with main pulses at 650–600 Ma, 580–550 Ma, ca. 530 Ma, 510–500 Ma, while post-500 Ma zircon U-Pb ages have not been reported so far (Elburg et al., 2016). The 650–600

Ma and 580–550 Ma events correspond to two main metamorphic episodes identified from elsewhere in this region, while 530–500 Ma thermal events are less prominent than in western-central DML. Pre-600 Ma magmatism in the SRM is represented by the Dufek granite in the SW Terrane, while combined new and previous data show that the granites in this area have a prolonged magmatic history with a broad range of ages at ca. 640 Ma (Elburg et al., 2016), ca. 620 Ma (Li et al., 2006), ca. 610 Ma to ca. 590 Ma (this study). The 580–550 Ma magma activity is characterized by bimodal magmatism, producing granites and minettes (Owada et al., 2013; Elburg et al., 2016). Neoproterozoic inheritance of 1000–900 Ma and 800–700 Ma are present (Elburg et al., 2016).

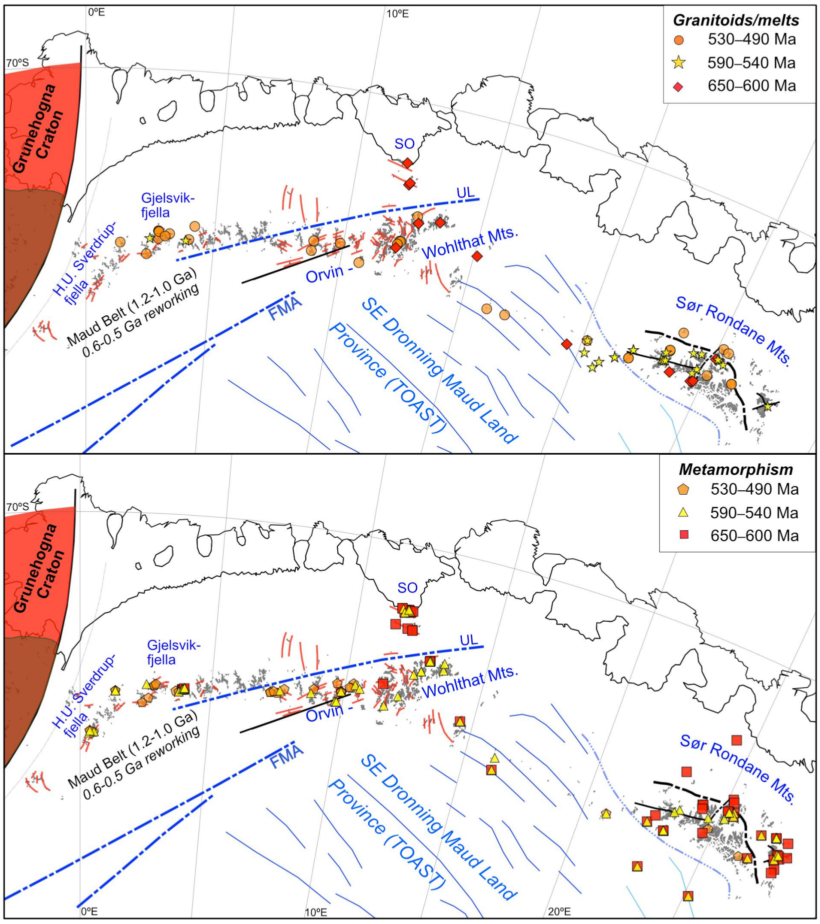

Fig. 9: Distribution of different magmatic and metamorphic age groups in DML. The detailed data list and sources are provided in tables 4 and 5, Supplementary File B. The abbreviations are the same as in Fig. 2.

5.2 Isotopic and geochemical perspective on magmatism in central DML

5.2.1 Late Neoproterozoic charnockite and anorthosite

Charnockites and anorthosites are mainly exposed in the easternmost part of the Orvin-Wohlthat Mountains (Fig. 2), and they commonly have significantly enriched (heavy) O isotopic compositions

($\delta^{18}O$=7.5–9.5 ‰) and slightly negative to positive εHf values (-1–+3). This implies that a considerable amount of older supracrustal material was most likely recycled into the magmas that generated 650–600 Ma magmas. Although some studies proposed that anorthosites are impossible to derive from purely crustal sources (e.g., Ashwal and Bybee, 2017), mantle-derived magmas are frequently contaminated by crustal components to various degrees during magma ascent. Enriched heavy O isotopes in anorthosites have been interpreted to be obtained from the assimilation of crustal components, or enriched sub-continental lithospheric mantle, or both. For example, Peck et al. (2010) reported 1.3 Ga Grenvillian anorthosites with high magmatic $\delta^{18}O$ (whole rock) values of 8–11‰ and attributed this to the involvement of oceanic crust during subduction; Heinonen et al. (2014) presented high $\delta^{18}O_{zrn}$ values (6.3–7.8 ‰) of 1.64 Ga Fennoscandian anorthosite that could be derived from the metasomatised subcontinental lithospheric mantle with a higher $\delta^{18}O$ value than the depleted mantle. In this study, it is possible that the mantle had been metasomatised by heavy $\delta^{18}O$ flux, which usually derived from the subducted oceanic slab, and contributed to enriched Hf and heavy O isotopic signatures of the 650–600 Ma charnockite-anorthosite magmas. However, the metasomatised mantle alone appears unable to produce a high enough shift in oxygen isotope as observed in this study (Eiler et al., 2000; Harris et al., 2015). An alternative explanation is that significant amounts of high $\delta^{18}O$ sedimentary material from the overlying crust were involved in 650–600 Ma magmas, and these sediments were originally from the subducted oceanic slab and attached to the lower crust of the eastern margin of the Kalahari Craton by subduction undeplating (Von Huene and Scholl, 1991). It is thus preferred here that high $\delta^{18}O$ crustal material played an important role in the formation of charnockite and anorthosite magmas, while the input of mantle-derived magma is uncertain, since its isotopic composition remains ambiguous.

5.2.2 Cambrian granitic and mafic rocks

The ca. 500 Ma quartz monzonite and granite samples in central DML generally show metaluminous and ferroan-potassic signatures. They have high incompatible trace element contents such as LREE, Zr and Nb, and plot in the field of A-type granites in the discrimination diagrams (Fig. 6). Most samples have a zircon-saturation temperature over 850°C (Fig. 6h), in line with the formation condition of typical A-type granites. The granitic rocks with these characteristics in major and trace element composition are classified as "ferro-potassic" (Fe-K) granitoids, which are generally formed during late- and post-collisional orogenic events (Ferré et al., 1998; Laurent et al., 2014; Terentiev and Santosh, 2018). However, their source composition, specifically the respective contribution from the mantle and crust-derived components, varies in different orogenic systems. Some studies ascribe its origin to the re-melting of pre-existing continental crust, either juvenile or old crust (e.g., Tagne-Kamga, 2003; Duchesne et al., 2010), while a derivation from metasomatised mantle with varying degrees of crustal contamination has also been proposed (e.g., Laurent et al., 2014).

The 500–485 Ma granitic samples from Gjelsvikfjella and the Orvin-Wohlthat Mountains in central DML show significantly evolved Hf isotopic compositions (Fig. 8a). The εHf (t) values of the samples from the latter region range from -10 to -5 corresponding to two-stage model ages between 2.0 and 1.8 Ga, while Hf compositions of some Gjelsvikfjella samples are more evolved with εHf (t) values of -15–-10 (Fig. 11d). One ca. 485 Ma gabbro (JT37) from Gjelsvikfjella has similarly unradiogenic Hf isotopic values (-14–-11) with the granitic rocks in this region. Their clear difference from 525 Ma mafic rocks in Hf isotopic composition indicates that the granitic and mafic rocks were derived from different sources, precluding the possibility that the granites were formed by the fractional crystallization of the mafic magmas. Furthermore, the paucity of mafic enclaves indicates that mafic additions and interaction with granitic magmas must have been insignificant, and the presence of Grenville-age and Neoproterozoic inherited zircons supports a large contribution from older continental crust. Some Gjelsvikfjella samples have even lower ε_{Hf} (t) values than the extrapolated Hf isotope values of the Grenville-age basement at ca. 500 Ma (Fig. 8a). This probably indicates an additional contribution of continental material that is isotopically more evolved than Grenville-age basement in this region, such as the Paleoproterozoic to Archean crust underlying the Kalahari Craton at its eastern side (Marschall et al., 2013; Wang et al., 2020). This indicates that older crust at the margin of the Kalahari Craton played a vital role in the genesis of the Cambrian post-collisional granitic magmas. Major element geochemistry of high-silica ferroan, calc-alkalic to alkali-calcic signatures of most samples indicate they were likely derived from anhydrous melting of intermediate metaigneous rocks under reducing conditions (Frost and Frost, 2008).

The ca. 500 Ma granitic samples from Gjelsvikfjella and the Orvin-Wohlthat Mountains show a clear difference in O isotopic signatures. The former is characterized by $\delta^{18}O$ values close to the mantle range, while the latter has higher $\delta^{18}O$ values at 7.0–8.0‰ (Fig. 7a). Their O isotopic compositions are interpreted as reflecting an inheritance from the Grenville-age basement in these two regions, as the O isotopic composition of the Grenville-age crust is generally mantle-like (5.5–6.0‰) in Gjelsvikfjella, whereas it is moderately higher than mantle value in the Orvin-Wohlthat Mountains (Wang et al., 2020).

The Nd isotope values of more than 40 granitic samples from central DML show a wide range from -14 to -3 with Nd model ages (T_{DM}) ranging from 2.1 to 1.4 Ga (Fig. 11b). In the εNd(t) vs. SiO_2 and trace element ratio diagrams (Fig. 10), the εNd(t) values appear to be broadly positively correlated to SiO_2 and negtively correlated to La/Sm, but no obvious correlation with other major elements and trace element ratios, such as MgO and Nd/Zr, is observed. This indicates that a simple two-endmember mixing model seems to be inappropriate to interpret the generation of granitic magmas here. Overall, the Cambrian granitic rocks probably derived from a mixture of multiple Precambrian crustal components, and the heterogeneous crustal compositions varied in different regions of central DML. For example, samples from the Conrad mountain, in the western part of the Orvin-Wohlthat Mountains, show significantly evolved Nd isotopic compositions with initial εNd values lower than -10 (Table 3 of Supplementary File C), more enriched than the recalculated Nd isotopic compositions of the Grenville-age basement to 500 Ma (Fig. 11b). In contrast, Holtedahlfjella samples generally have εNd(t) values of -6–-4, which are in the range of the εNd(t) values of the Grenville-age basement at ca. 500 Ma (Fig. 11b). The complexity of the continental crust in central DML is also revealed by isotopic compositions of the Grenville-age basement rocks, as they exhibit both juvenile and highly evolved Hf and Nd isotopes, indicating the co-existence of juvenile Mesoproterozoic crust and older crustal components (Wang et al., 2020).

The ca. 525 Ma gabbro and lamprophyre dyke (J1826, 2312-2) yield a more radiogenic Hf isotopic composition than ca. 500 Ma granitic samples but with negative εHf values of -4– -2, which can be explained either as their primitive melts derived from an enriched mantle source (lithospheric mantle metasomatized by recycled crustal materials) or melts derived from the depleted (asthenospheric) mantle with significant crustal contamination. These samples (SiO_2 = 43–50%) are enriched in compatible elements (Fe, Mg, Cr, Ni), and have a low content of incompatible elements (K_2O, HFSE, LREE), which makes the first explanation more likely although crustal contamination cannot be excluded. This is consistent with a previous study (Owada et al., 2008) that interprets similarly-aged lamprophyre and lamproite rocks in the Mühlig-Hofmann Mountains to have derived from the enriched mantle. In addition, enriched Sr–Nd–Pb–O isotopic compositions of ca. 455 Ma minettes from the Schirmacher Oasis also indicate the existence of metasomatized lithospheric mantle beneath central DML (Hoch et al., 2001), although when and how mantle enrichment took place remains uncertain. Recent modelling reveals that post-collisional (ultra)mafic magmatism largely originated from a mantle source, which, however, is often not reflected by Hf–O isotopic compositions, since even a small proportion (10–20%) of continental material or melts/fluids generated from them interacting with the mantle would drive Hf isotopic composition to a crust-like signature and also O isotope above the mantle value (Couzinié et al., 2016). Therefore, we prefer to interpret the ca. 525 Ma mafic magmas to have been derived from an enriched mantle source that most likely acquired its enriched isotopic composition during the Precambrian subduction events.

In summary, the isotopic and geochemical data presented here support the view that ca. 500 Ma granitic rocks in central DML were largely derived from the remelting of pre-existing continental crust, while the ca. 525 Ma mafic magmas, which have more radiogenic Hf isotopes, most likely derived from an enriched mantle source that was metasomatised by earlier subduction processes. This is typical for postorogenic and post-collisional magmatism (Bonin, 2004).

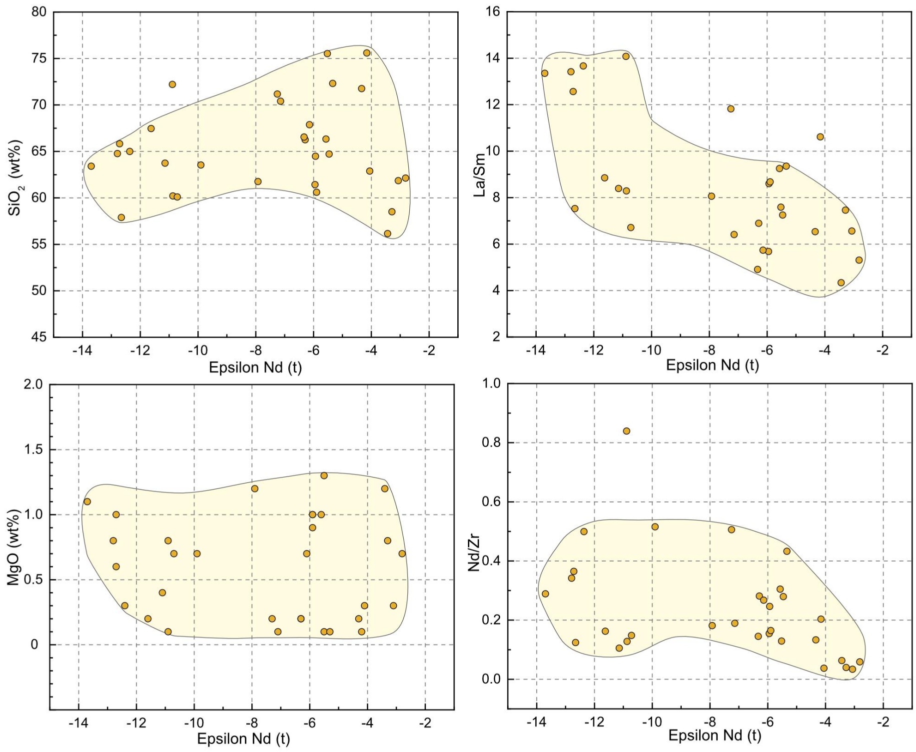

Fig. 10: Initial εNd values versus SiO_2, MgO, La/Sm and Nd/Zr of Cambrian granitic samples from the Orvin-Wohlthat Mountains (central DML). The light yellow fields show the range of the majority of the analysed samples.

5.3 Isotopic signatures of granites in eastern DML

The Hf and Nd isotopes of 650–500 Ma granites from the SRM exhibit overall more juvenile signatures than synchronous samples from central DML (Fig. 11b, c). Their εHf (t) values are dominantly between -5 and +5 (this study; Elburg et al., 2016), and the array of them, especially for the pre-540 Ma samples, broadly follows the evolution trend of GTTGs of the TOAST (Fig. 8b). They have slightly negtive εNd (t) values of -3–-1 and late Mesoproterozoic Nd model ages, in contrast to the significantly negtive εNd (t) values and Archean to Paleoproterozoic model ages of most central DML samples (Fig. 11b). The $\delta^{18}O$ values are mostly between 6 and 7‰, more 'mantle-like' than samples from the eastern part of central DML (Fig. 7b). These differences in Hf–Nd–O isotopes are closely related to the varying isotopic signatures of the Precambrian basement from west to east. Compared to the Grenville-age basement in western-central DML (Fig. 8a), the TOAST rocks overall have more homogeneous and juvenile Hf isotopic compositions with most εHf (t) values of +5–+10 (Fig. 8b), and an average of mildly elevated $\delta^{18}O$ value at around 6.5‰ (sample J1212E, Fig. 7b).

Hf and Nd isotopic compositions as well as whole-rock geochemistry of the granites in eastern DML show a variation from late Neoproterozoic to Cambrian times. The Ediacaran samples generally have suprachondritic Hf and Nd isotope signatures, while the post-540 Ma granites have a more evolved radiogenic isotopic composition with negative εHf (t) and εNd (t) values (Fig. 11b-c). The initial εHf values of ca. 600–500 Ma granites in this study display a trend that gradually decreases and deviates from the secular evolution of TOAST crust (Fig. 8b), and a similar isotopic pattern is also revealed by Elburg et al. (2016). This can be interpreted as the increasing involvement of pre-existing, old continental material, especially for the post-540 Ma samples. In addition, a higher SiO_2 concentration and lower alkalic geochemistry as well as higher zircon saturation temperatures observed in Cambrian rocks compared to older samples (Fig. 6a-c, h) is consistent with the formation of the former by remelting more continental material. It is not excluded that juvenile input may have played a considerable role in the formation of the late Neoproterozoic granites, its contribution, however, diminished in Cambrian times.

The 570–550 Ma igneous activity in the SRM produced coeval lamprophyre dykes, minettes and syenites (Lunckeryggen) at ca. 560 Ma, which have evolved Nd isotopic composition (εNd (t) values around 0) and have been interpreted as derived from an enriched mantle (Li et al., 2003, 2006; Owada et al., 2008, 2013). These rocks were further interpreted to have formed under an extensional setting with an elevated geothermal gradient due to the upwelling of the asthenosphere and thinning of the lithosphere (Owada et al., 2013). In this study, however, high silica concentration, neutral εHf (t) and mildly elevated $\delta^{18}O$ values (7%) of 560–555 Ma samples (Fig. 7) suggest that these granitic magmas contain significant involvement of crustal components of the TOAST. The relevant post-530 Ma samples are distributed across SE DML and the SW Terrane of the SRM, and a broad trend that the εHf (t) values are more unradiogenic from west to east was revelaed by Elburg et al. (2016). In this study, two granites from SE DML yield higher $\delta^{18}O$ values (7.5–8 ‰) than samples from the SRM (<7 ‰) (Fig. 11c). The varied Hf and O isotopes of the Cambrian granites in eastern DML probably indicate different source regions of old continental components, which could be from the Kalahari Craton, Indo-Antarctica or the Valkyrie Craton (Fig. 2).

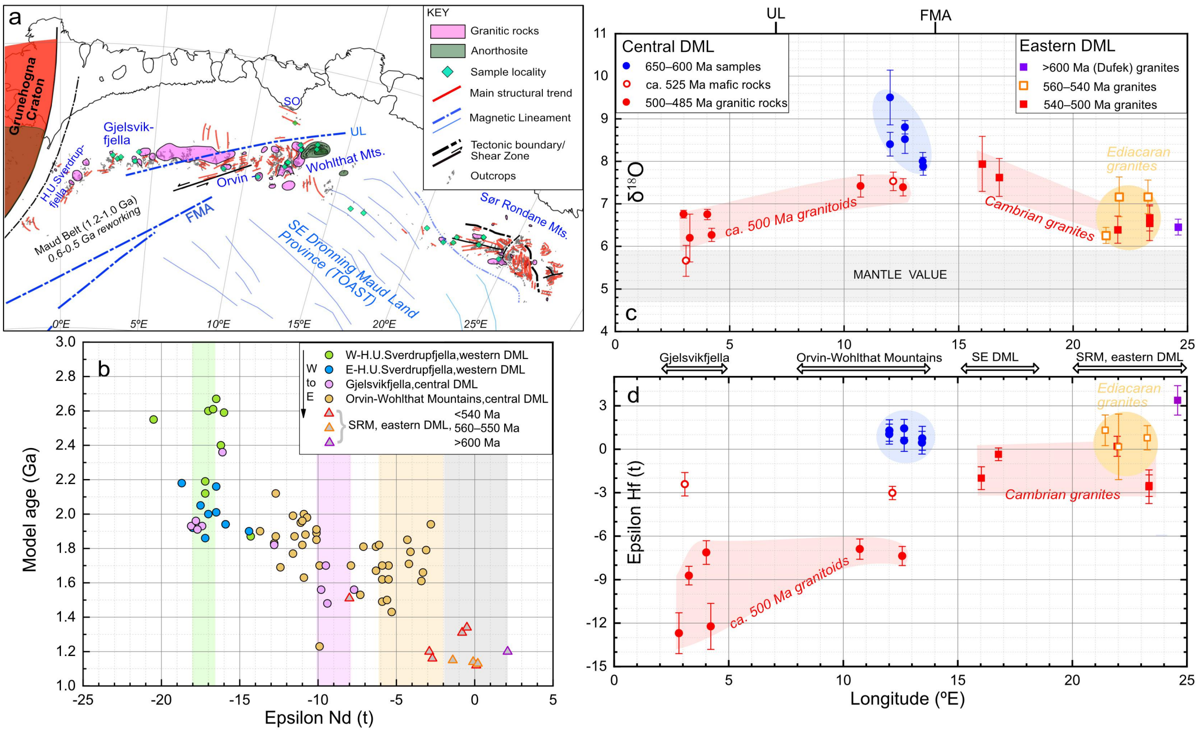

Fig. 11: (a) Geological overview map of DML and sampled Hf-O isotopic profile along the DML mountain range; (b) Nd model ages versus initial epsilon values of Cambrian granitic samples from H.U. Sverdrupfjella (western DML) across central DML to SRM (Table 3 in Supplementary File C). The Nd isotopic data of H.U. Sverdrupfjella, Gjelsvikfjella and the Orvin-Wohlthat Mountains are from Moyes (1993), Moyes et al. (1993b), Paulsson and Austrheim (2003), Markl and Henjes-Kunst (2004), Grantham et al. (2019) and this study; the Nd isotopic data of eastern DML are from Jacobs et al. (2015) and this study; the light green, purple yellow and gray bars indicate the range of εNd (t) values of the Precambrian basement in H.U. Sverdrupfjella, Gjelsvikfjella, the Orvin-Wohlthat Moutains and eastern DML respectively when calculated at Cambrian times (Table 4 in Supplementary File C); Sm-Nd isotopic data of basement rocks are from Moyes (1993), Wareham et al. (1998), Paulsson and Austrheim (2003), Jacobs et al. (1998), Kamei et al. (2013), Jacobs et al. (2015) and Elburg et al. (2015); (c-d) O and Hf isotopic composition and variation from Gjelsvikfjella to SRM, see text for detailed explanations.

5.4 Tectonic evolution in DML during Gondwana assembly

Our new zircon U–Pb–Hf–O and whole-rock Nd isotopic data provide detailed insights into the protracted tectonic processes of two major crustal domains, western-central DML and eastern DML that are separated by the Forster Magnetic Anomaly. Western-central DML is underlain by Grenville age basement, whilst eastern DML is underlain by the TOAST. In late Neoproterozoic times, the two crustal domains largely record different crustal evolutions, whilst from ca. 590 Ma onwards the geological processes overall record a common tectono-metamorphic history, reflected by commonly extensive high-grade metamorphism, migmatisation and granitic magmatism (Fig. 9).

In western-central DML, evidence for a retreating accretionary continental margin comes from 650–600 Ma charnockites, anorthosites and granodiorites at the eastern periphery of the Kalahari Craton, close to the Forster Magnetic Anomaly. These igneous rocks commonly have highly elevated O (8–9‰) and radiogenic Hf isotopic compositions (εHf(t) = 0–+2), distinct from the significantly unradiogenic Hf and mantle-like to moderately high O isotopic values of the later Cambrian granitic rocks (Fig. 11c, d). This demonstrates that the sources they were derived from are different. The 650–600 Ma magmas most likely involved significant amounts of high $\delta^{18}O$ sedimentary components at the eastern margin of the Kalahari Craton. The eastern margin of the Kalahari Craton has been an active continental margin in the Neoproterozoic, such as during late Tonian times, at ca. 785–760 Ma (e.g., Jacobs et al., 2020). The eastern Kalahari Craton margin repeatedly changed from an advancing to a retreating continental margin and vice verca during the Neoproterozoic. The ca. 650 Ma charnockite magmatism (J1883, this study) is accompanied by UHT metamorphism (950–1050 ºC, 0.9–1.0 GPa, Baba et al., 2006, 2010) in the Schirmacher Oasis, probably indicating subduction rollback and a back-arc environment (e.g., Baba et al., 2010; Jacobs et al., 2020). The formation of 610–600 Ma anorthosites, charnockites and granodiorites accompanied by high-grade metamorphism recorded by metamorphic zircon rims (Jacobs et al., 2020 and unpublished data) may relate to the inversion of the back-arc basin.

In western-central DML, the Nd isotopic compositions of Cambrian granitic rocks exhibit a clear spatial variation from H.U. Sverdrupfjella (western DML) to the Orvin-Wohlthat Mountains (central DML) (Fig. 11b), indicating that the composition and/or proportion of involved crustal components have varied significantly. The westernmost part of western DML (western H.U. Sverdrupfjella) is characterised by Archean Nd model ages of 2.7–2.5 Ga, while samples from eastern H.U. Sverdrupfjella and Gjelsvikfjella mostly yield Paleoproterozoic model ages. Further east, Nd model ages of samples from the Orvin-Wohlthat Mountains have a wide range from 2.1 to 1.4 Ga (Fig. 11b).

The trend that Nd isotopes are increasingly more radiogenic towards the east (towards the margin of the Kalahari Craton) is consistent with the regional trends of the Hf and Nd isotope signatures of the Grenville-age basement (Wang et al., 2020), although the Nd isotopic compositions of part of the Cambrian intrusions in central DML appear to be more enriched than those of the Grenville-age basement calculated at Cambrian times (Fig. 11b). In contrast, the ca. 525 Ma mafic magmas (garbbros and lamprophyres), which have more juvenile Hf isotopic signatures than the voluminous ca. 500 Ma granitic rocks, are most likely derived from an enriched mantle source. This magma formation mechanism supports the tectonic process proposed by previous studies, that the delamination of an orogenic root removed part of the lithospheric mantle and induced extensive melting in the upper lithospheric mantle and in the continental crust, producing large-scale post-collisional magmatism (Jacobs et al., 2003b, 2008). The magmas that gave rise to the restricted ca. 525 Ma mafic rocks in central DML probably formed at the start of lithosphere mantle delamination, while the widespread post-collisional magmatism that re-melted the overlying continental crust occurred subsequently at ca. 500 Ma.

In eastern DML, the Ediacaran-Cambrian granites have unsurprisingly more radiogenic Hf–Nd isotopic compositions (Fig. 11b, 11d), as the Tonian basement in eastern DML (TOAST) is more juvenile than the Grenville-age crust in central DML (Fig. 8). The radioactive isotope composition of the granites from eastern DML is characterised by a dramatic decrease in Hf and Nd isotopic values of Cambrian granites compared with older samples, which indicates the increased involvement of evolved continental material after 540 Ma. The juvenile Hf isotopes of the 640–600 Ma Dufek granites indicate that the TOAST was rather isolated in the Mozambique Ocean with very limited input of old continental crustal in early Ediacaran times. It clearly developed on an independent subduction system than the synchronous subduction system at the periphery of the eastern Kalahari Craton. The subduction system that affected the TOAST was contractional as evident by the overthrusting of the NE Terrane onto the SW Terrane in the SRM (e.g., Adachi et al., 2013). The increasing input of older crustal components after ca. 540 Ma suggests that the TOAST had become wedged between adjacent older cratons latest by Cambrian times. The subsequent delamination and orogenic collapse, which mainly happened in central DML, also influenced eastern DML to some extent and resulted in the Cambrian magmatism.

Western-central and eastern DML obviously underwent different crustal evolutions before ca. 590 Ma and were not joint by that time. However, subsequent 590–550 Ma high-grade metamorphism and migmatisation is widespread and quite uniform across entire DML (Fig. 9), including the Lützow-Holm Bay to the east (Tsunogae et al., 2014, 2015). This tectono-metamorphic episode most likely represents the main period of crustal thickening in the southern part of the EAAO, during which various cratons and terranes, including the Kalahari Craton, the TOAST, Indo-Antarctica and probably the Valkyrie Craton finally amalgamated (Fig. 12). This scenario is consistent with the tectonic evolution in the central EAAO. Recent work on the 580–540 Ma high-grade metamorphism such as in Madagascar and south India suggests that the intervening Mozambique Ocean were not completely closed until ca. 550 Ma or even later (Armistead et al., 2020; Boger et al., 2015; Yeshanew et al., 2017; Clark et al., 2020). Thus, in late Neoproterozoic times, DML is dominated by E-W oriented (present coordinates) convergent tectonics that led to the final closure of the Mozambique Ocean at the transition from Neoproterozoic to Cambrian times. Post-collisional delamination and collapse caused widespread magmatism and associated metamorphism in an overall extensional setting. The late Neoproterozoic to Cambrian rocks in DML thus record an orogenic cycle from subduction-accretion, continental collision to post-collisional process during and after the assembly of Gondwana.

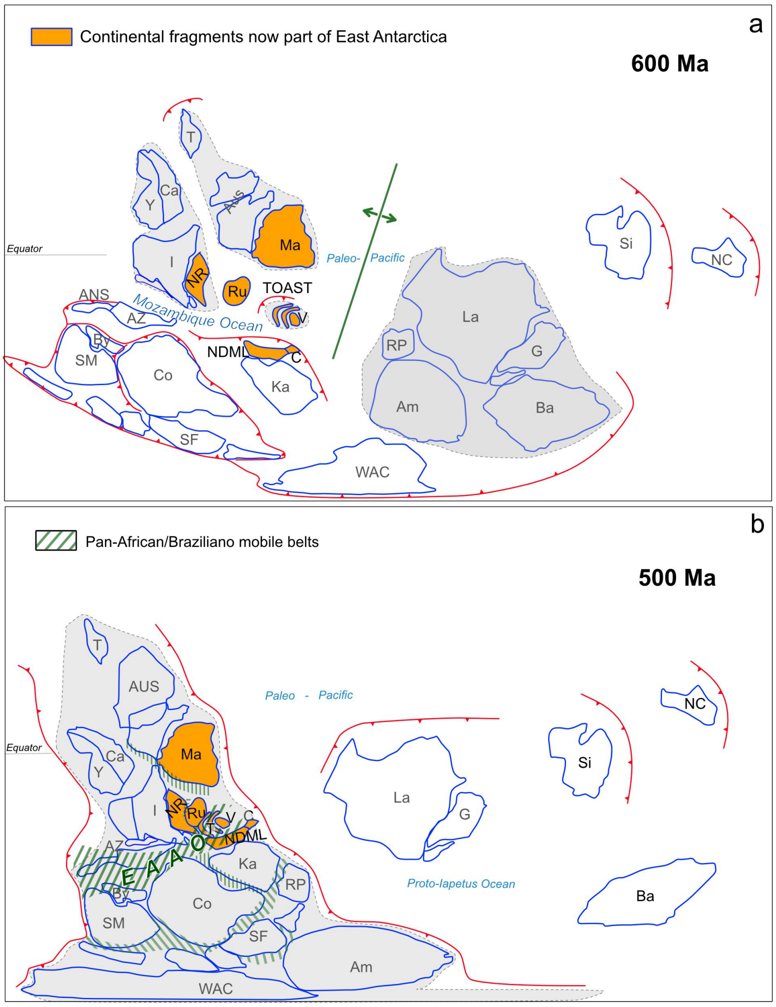

Fig. 12: Continental reconstructions at 600 and 500 Ma, indicating the various East Antarctic continental fragments (orange) with African, Australian, Indian and Laurentian heritage as well as juvenile crust such as the TOAST that joined during the assembly of Gondwana (based and modified after Merdith et al., 2017). a) By 600 Ma the Paleo-Pacific is still expanding, whilst the Mozambique Ocean is near to closure. Different parts of DML are characterized by different subduction zone systems, probably no continental collision so far. b) By 500 Ma, Gondwana had assembled along a network of Pan-African/Braziliano mobile belts, of which the East African-Antarctic Orogen (EAAO) appears to be one of the major ones, stretching from the Arabian Nubian Shield, along East Africa into East Antarctica. In DML, the best age estimate for continental collision between the Kalahari Carton, the TOAST, the Ruker Craton and an Indo-Antarctic block is ca. 590–550 Ma. Abbreviations: Am, Amazonia; Aus, Australia; AZ, Azania; Ba, Baltica; By, Bayuda block; SC, South China; C, Coats Land Block; Ca, Cathaysia; Co, Congo; G, Greenland; I, India; Ka, Kalahari; La, Laurentia; M, Madagascar; Ma, Mawson; NC, North China; NDML, Nampula-Dronning Maud Land (western-central); NR, Napier-Rayner (Antarctica); RP, Rio de la Plata; Ru, Ruker Craton, SF, Sao Francisco; Si, Siberia; SM, Sahara

Metacraton; TOAST, Tonian Oceanic Arc Super Terrane; V, Valkyrie Craton; WAC, West African Craton; Y, Yangtze.

Summary and conclusions

DML preserves an extensive record of late Neoproterozoic–Cambrian magmatic and metamorphic activity associated with the closure of the Mozambique Ocean and the assembly of Gondwana. New and compiled published geochronology data indicate that central and eastern DML have distinct magmatic and metamorphic history and probably did not join before ca. 590–550 Ma. In late Neoproterozoic times (ca. 650–600 Ma), central DML formed a retreating accretionary continental margin along the eastern Kalahari Craton with extensive records of anorthosite and charnockite magmatism and accompanied UHT metamorphism. In contrast, eastern DML records granite magmatism, crustal stacking and associated granulite facies metamorphism at the same time that probably resulted from the collision of the TOAST with the Valkyrie Craton. Common pervasive tectono-metamorphism of central and eastern DML is recorded from ca. 590 Ma onwards, although the associated magmatic record differs somewhat in the two broadly different regions. Whilst eastern DML records long-term and continuous magmatism from ca. 650 to 500 Ma, central DML is dominated by voluminous late-tectonic magmatism between ca. 530–485 Ma.

The 650–600 Ma anorthosite and charnockite samples in easternmost central DML (eastern periphery of the Kalahari Craton) have slightly positive εHf(t) (0–+2) and heavy $\delta^{18}O$ values (8–9‰), indicating a large involvement of high $\delta^{18}O$ crustal components. The reason for this is likely that the long-term active continental margin setting of the easternmost Kalahari Craton allowed for the addition of sedimentary material. The initial Cambrian magmatism in central DML is marked by mafic magmas at ca. 525 Ma, followed by very voluminous granitic magmas across the entire region between ca. 510–485 Ma. The granitic rocks generally have enriched Hf isotopic compositions with εHf(t) values of -10–-6 and mildly elevated $\delta^{18}O$ values. Their Nd isotopes show a regional variation towards radiogenic values from west to east, with model ages varying from the Archean to Mesoproterozoic, which is consistent with the isotopic trend of the Grenville-age crust in this region. As such, the Cambrian granitic magmas are interpreted to have mainly derived from the re-melting of pre-existing continental crust.

Compared to the Cambrian granitic rocks from central DML, the late Neoproterozoic-Cambrian granites from the SRM of eastern DML have more juvenile Hf isotopic compositions associated with O values closer to the mantle range, which points to a distinct source, most likely the TOAST crust. The 640–600 Ma granites in eastern DML (Dufek granites) have more juvenile Hf and Nd isotopic compositions than the post-540 Ma granites, indicating that the TOAST crust was in the vicinity of, and probably had been sandwiched in between, other continental fragments by Cambrian times. The increasingly negative εHf(t) values in the Cambrian are interpreted to document the change in tectonic setting from subduction accretion to continental collisions.

Therefore, the first detailed zircon U–Pb–Hf–O and new whole-rock Nd isotopic data of late Neoproterozoic to Cambrian igneous rocks in western-central and eastern DML provide a significantly improved understanding of the tectonic setting that led to the amalgamation of DML and East Antarctica. It is significant to note that the eastern margin of Kalahari and the TOAST developed on two independent subduction systems in late Neoproterozoic times. The accretion and assembly of the TOAST to the Kalahari Craton and collision with surrounding continental blocks (i.e. Indo-Antarctica and Valkyrie Craton) probably happened in late Ediacaran times, which marks the closure of the Mozambique Ocean and the amalgamation of Gondwana. Subsequently, DML was affected by extensive post-collisional magmatism due to delamination tectonics and orogenic collapse in Cambrian times, resulting in voluminous A-type granitic rocks, which generally have crustal characteristics as revealed by their isotopic and geochemical signatures.

Acknowledgements

This work was financially supported by faculty-specific funds and endowments of the Faculty of Mathematics and Natural Sciences, University of Bergen (NO. 812378), and was partly supported by the Research Council of Norway through the funding to The Norwegian Research School on Dynamics and Evolution of Earth and Planets (NO. 249040/F60). C-C. Wang is grateful to the support from the China Scholarship Council. J. Jacobs thanks for continued field support of the Alfred-Wegener Institute Helmhotz Centre of Polar and Marine Research (AWI) Bremerhaven, the

Federal Institute for Geosciences and Natural Resources (BGR), Hannover and the Norwegian Polar Institute, Tromsø. N.W. Roland is thanked for providing samples from central DML for Sm–Nd isotopic analyses. We thank I.C. Kleinhanns for providing unpublished major and trace element (eastern DML) and Sm–Nd isotope data (central and eastern DML). We thank M. Whitehouse and his team for their help with SIMS zircon U–Pb–O isotopic analyses, P. Montero and F. Bea for their help with SHRIMP U–Pb–O analyses. The MC-ICP-MS lab at UJ was funded by NRF-NEP grant 93208, and is supported by DSI-NRF CIMERA. M. A. Elburg acknowledges NRF IFRR funding (No. 119297). Two anonymous reviewers are thanked for their constructive and insightful comments that greatly improved the quality of the manuscript. We thank editor V. Pease for her efficient handling of this paper. This is IBERSIMS publication #XX and NORDSIM publication #XXX.

Table 1. Summary of analysed samples from central and eastern DML in this study.

Sample	Latitude (S)	Longitude (E)	Rock types	Main mineral composition	Zircon characterization	Th, U concentration and Th/U ratio of concordant igneous analyses	Igneous age (Ma) (# of conc. igneous analyses / # of total)	Inherited ages (Ma)	εHf (t)	Model age (Ga)	$\delta^{18}O$ (‰)
Gjelsvikfjella, central DML (530-485 Ma)											
2312-2[1]	-72.000373	3.088794	Lamprophyre dyke	Pl, Kfs, Bt, Qtz			ca. 525		-2.4 ± 1.6		5.8 ± 0.7
JT19[a]	-72.024676	4.025192	Charnockite	Opx, Amp, Pl, Kfs, Qtz	subhedral to euhedral, 100–250 µm, oscillatory zoning	40–170, 130–520, 0.3–0.4	500 ± 3 (13/14)		-7.1 ± 1.6	1.83–1.99	6.8 ± 0.5
JT22[a]	-71.861973	4.215732	Granite	Kfs, Qtz, Pl	subhedral to euhedral, 200–300 µm, oscillatory zoning	60–700, 110–1750, 0.1–1.8	499 ± 4	ca. 1080	-12.2 ± 2.0	2.06–2.36	6.3 ± 0.6
3112-2[1]	-71.969864	3.263118	Granite	Kfs, Pl, Bt, Qtz			487 ± 4		-8.7 ± 1.3	1.94–2.04	6.3 ± 0.9
JT37[a]	-71.941944	2.826667	Gabbro (Stabben)	Bt, Amp, Pl, Cpx	small, irregular, weak zoning	50–170, 50–230, 0.9–1.5	483 ± 4 (8/10)	ca. 1090	-12.7 ± 2.1	2.07–2.39	6.8 ± 0.4
Orvin-Wohlthat Mountains, central DML (530-485 Ma)											
J1826[b]	-71.690620	12.145744	Gabbro	Amp, Bt, Pl, Qtz, Cpx	euhedral, up to 500 µm, oscillatory zoning	40–430, 90–380, 0.5–1.1	524 ± 2 (16/21)		-3.0 ± 0.9		8.0 ± 0.4
J1870[2]	-72.038188	10.721204	Charnockite	Pl, Kfs, Qtz, Opx, Amp, Bt			501 ± 7		-6.9 ± 1.4	1.81–1.93	7.4 ± 0.5
J1670[2]	-71.352218	12.575029	Granite	Kfs, Pl, Qtz, Amp			499 ± 4		-7.4 ± 1.4	1.81–1.93	7.4 ± 0.4
J1821[c]	-71.689233	12.099042	Charnockite	Opx, Pl, Qtz	oscillatory zoning		514 ± 5 (39/52)	ca. 1068, 600			
J1825[c]	-71.689233	12.099042	Syenite	Kfs, Pl, Bt, Amp	oscillatory zoning		494 ± 6 (15/23)	ca. 1058, 600			
J1684[c]	-71.991797	8.816522	Granite	Kfs, Qtz, Pl, Bt, Amp	oscillatory zoning		486 ± 7 (16/23)	ca. 1065, 610			
Orvin-Wohlthat Mountains, central DML (650-600 Ma)											
J1883[b]	-71.431244	12.659893	Charnockite	Pl, Qtz, Kfs, Opx, Bt, Amp	subhedral or irregular, 150–250 µm, oscillatory zoned cores- srructureless rims	20–90, 70–250, 0.3–0.5	645 ± 6 (8/29)		+1.2± 1.1	1.38–1.52	8.8 ± 0.3

J1848[b]	-71.775703	12.010605	Gt-gneiss	Kfs, Pl, Qtz, Bt, Grt	a mixture of large (700 µm) and smaller zircons (generally between 200–350 µm), oscillatory zoned cores-srructureless mantle and rims	50–130, 170–430, 0.3–0.5	636 ± 7 (5/33)		+1.1± 1.4	1.43–1.53	8.4 ± 0.6
J1886[3]	-71.431244	12.659893	Charnockite	Pl, Qtz, Kfs, Opx, Amp			608 ± 9		+0.6± 1.5	1.41–1.58	8.5 ± 0.7
J1955[3]	-71.364170	13.449743	anorthosite	Pl, Opx, Amp, Qtz			600 ± 12		+0.9± 1.6	1.38–1.57	7.9 ± 0.4
J1958[3]	-71.282666	13.436036	anorthosite	Pl, Opx, Amp, Qtz			583 ± 7		+0.5± 1.6	1.43–1.57	8.5 ± 0.7
SE DML											
SG 27[4]	-72.234169	16.774981	Granodiorite	Pl, Kfs, Qtz, Bt, Amp			532 ± 5	ca. 730	-0.4 ± 0.9	1.46–1.53	7.5 ± 0.9
SG 24[4]	-72.223950	16.027433	Granite	Kfs, Pl, Qtz, Bt			503 ± 5		-2.0 ± 1.6	1.48–1.65	7.9 ± 1.3
SRM, eastern DML											
J1212E[4]	-72.150050	20.321083	Amphibole gneiss	Qtz, Pl, Kfs, Bt, Amp, Ms			925 ± 11		+5.5 ± 1.7	1.35–1.54	6.6 ± 0.5
TC46[b]	-72.195043	23.650854	Dufek Granite	Kfs, Pl, Qtz, Bt	subhedral to euhedral, 200–400 µm, oscillatory zoned cores and thin, CL-dark rims	210–600, 380–1000, 0.3–0.9	606 ± 1 (6/20)				
TC41[b]	-72.196507	24.593602	Dufek Granite	Kfs, Pl, Qtz, Bt	subhedral to euhedral, 150–300 µm, oscillatory zoned cores and CL-dark, structureless rims	100–150, 100–300, 0.3–0.7	588 ± 4 (7/22)		+3.0 ± 2.0	1.21–1.41	6.5 ± 0.8
J1214B[4]	-72.284683	21.435233	Granite	Kfs, Pl, Qtz, Amp, Bt			557 ± 2		+1.0 ± 2.2	1.32–1.48	6.1 ± 0.8
J1216B[4]	-72.121600	22.018700	Quartz-monzonite	Kfs, Pl, Qtz, Bt			555 ± 4	ca. 600, 750, 850	-0.5 ± 5.2	1.36–1.59	6.7 ± 1.5
23A-1[a]	-72.100100	23.269733	Granite	Kfs, Pl, Qtz, Bt	euhedral, 200–300 µm, oscillatory zoning	100–600, 200–800, 0.3–0.9	555 ± 4 (8/10)	ca. 620	+1.0 ± 0.7	1.35–1.46	7.2 ± 0.8
J1216A[4]	-72.228930	21.953620	Granite	Kfs, Pl, Qtz, Bt			534 ± 4		+0.1 ± 1.0	1.36–1.53	6.4 ± 0.6
20A-1[a]	-71.946691	23.344872	Granite	Kfs, Pl, Qtz, Bt	euhedral, 300–400 µm, oscillatory zoning	30–170, 120–540, 0.3–0.5	524 ± 3 (9/12)		-3.2 ± 1.6	1.49–1.73	6.6 ± 0.8
19A-1[a]	-71.954113	23.349175	Granite	Kfs, Pl, Qtz, Bt	euhedral, 300–400 µm, oscillatory zoning	40–170, 130–520, 0.3–0.4	521 ± 2 (13/15)		-2.5 ± 1.5	1.54–1.68	6.7 ± 0.6

Samples in each region are ordered by age. The samples with superscript a and b are newly dated samples in this study, a-SIMS, b-SHRIMP; c-LA-ICP-MS (Suliman, 2011).

1-Jacobs et al., 2003a, 2- Jacobs et al., 2008a, 3- Jacobs et al., 1998, 4- Jacobs et al., 2015, all are SHRIMP ages; Mineral abbreviations from Whitney and Evans (2010).

References

Adachi, T., Osanai, Y., Hokada, T., Nakano, N., Baba, S., Toyoshima, T., 2013. Timing of metamorphism in the central Sør Rondane Mountains, eastern Dronning Maud Land, East Antarctica: Constrains from SHRIMP zircon and EPMA monazite dating. Precambrian Research 234, 136–160.

Archibald, D.B., Collins, A.S., Foden, J.D., Payne, J.L., Holden, P., Razakamanana, T., 2019. Late syn-to post-collisional magmatism in Madagascar: The genesis of the Ambalavao and Maevarano Suites. Geoscience Frontiers 10, 2063–2084.

Armistead, S.E., Collins, A.S., Redaa, A., Jepson, G., Gillespie, J., Gilbert, S., Blades, M.L., Foden, J.D., Razakamanana, T., 2020. Structural evolution and medium-temperature thermochronology of central Madagascar: implications for Gondwana amalgamation. Journal of the Geological Society.

Ashwal, L.D., Bybee, G.M., 2017. Crustal evolution and the temporality of anorthosites. Earth-Science Reviews 173, 307–330.

Baba, S., Owada, M., Grew, E.S., Shiraishi, K., 2006. Sapphirine granulite from Schirmacher Hills, central Dronning Maud Land. In: Fütterer, D.K., Damaske, D., Kleinschmidt, G., Miller, H., Tessensohn, F. (Eds.), Antarctic Contributions to Global Earth Science. Springer, Berlin, pp. 37–44.

Baba, S., Owada, M., Shiraishi, K., 2008. Contrasting metamorphic P–T path between Schirmacher Hills and Mühlig-Hofmannfjella, central Dronning Maud Land, East Antarctica. Geological Society, London, Special Publication 308, 401–417.

Baba, S., Hokada, T., Kaiden, H., Dunkley, D.J., Owada, M., Shiraishi, K., 2010. SHRIMP zircon U-Pb dating of sapphirine-bearing granulite and biotite-hornblende gneiss in the Schirmacher Hills, east Antarctica: implications for Neoproterozoic ultrahigh-temperature metamorphism predating the assembly of Gondwana. The Journal of Geology 118, 621–639.

Baba, S., Osanai, Y., Nakano, N., Owada, M., Hokada, T., Horie, K., Adachi, T., Toyoshima, T., 2013. Counterclockwise P–T path and isobaric cooling of metapelites from Brattnipene, Sør Rondane Mountains, East Antarctica: implications for a tectonothermal event at the proto-Gondwana margin. Precambrian Research 234, 210–228.

Baba, S., Horie, K., Hokada, T., Owada, M., Adachi, T., Shiraishi, K., 2015. Multiple collisions in the East African–Antarctica Orogen: constraints from timing of metamorphism in the Filchnerfjella and Hochlinfjellet terranes in central Dronning Maud Land. The Journal of Geology 123, 55–77.

Bingen, B., Jacobs, J., Viola, G., Henderson, I.H.C., Skår, Ø., Boyd, R., Thomas, R.J., Solli, A., Key, R.M. and Daudi, E.X.F., 2009. Geochronology of the Precambrian crust in the Mozambique belt in NE Mozambique, and implications for Gondwana assembly. Precambrian Research 170, 231–255.

Bisnath, A., Frimmel, H.E., 2005. Metamorphic evolution of the Maud Belt: P–T–t path for high-grade gneisses in Gjelsvikfjella, Dronning Maud Land, East Antarctica. Journal of African Earth Sciences 43, 505–524.

Bisnath, A., Frimmel, H.E., Armstrong, R.A., Board, W.S., 2006. Tectono-thermal evolution of the Maud Belt: new SHRIMP U–Pb zircon data from Gjelsvikfjella, Dronning Maud land, East Antarctica. Precambrian Research 150, 95–121.

Boehnke, P., Watson, E.B., Trail, D., Harrison, T.M., Schmitt, A.K., 2013. Zircon saturation re-revisited. Chemical Geology 351, 324–334.

Boger, S.D., 2011. Antarctica—before and after Gondwana. Gondwana Research 19, 335–371.

Boger, S.D., Hirdes, W., Ferreira, C.A.M., Jenett, T., Dallwig, R., Fanning, C.M., 2015. The 580–520 Ma Gondwana suture of Madagascar and its continuation into Antarctica and Africa. Gondwana Research 28, 1048–1060.

Board, W.S., Frimmel, H.E., Armstrong, R.A., 2005. Pan-African tectonism in the western Maud Belt: P–T–t path for high-grade gneisses in the H.U. Sverdrupfjella, East Antarctica. Journal of Petrology 46, 671–699.

Bonin, B., 2004. Do coeval mafic and felsic magmas in post-collisional to withinplate regimes necessarily imply two contrasting, mantle and crustal, sources? A review. Lithos 78, 1–24.

Bouvier, A., Vervoort, J.D., Patchett, P.J., 2008. The Lu–Hf and Sm–Nd isotopic composition of CHUR: constraints from unequilibrated chondrites and implications for the bulk composition of terrestrial planets. Earth and Planetary Science Letters 273, 48–57.

Clark, C., Collins, A.S., Taylor, R.J., Hand, M., 2020. Isotopic systematics of zircon indicate an African affinity for the rocks of southernmost India. Scientific Reports 10, 1–12.

Collins, A.S., Pisarevsky, S.A., 2005. Amalgamating eastern Gondwana: the evolution of the Circum-Indian Orogens. Earth Science Reviews 71, 229–270.

Colombo, F., Talarico, F. 2004. Regional metamorphism in the high-grade basement of central Dronning Maud Land, East Antarctica. Geologisches Jahrbuch, Reihe B, 96, 7–47.

Couzinié, S., Laurent, O., Moyen, J.F., Zeh, A., Bouilhol, P., Villaros, A., 2016. Post-collisional magmatism: crustal growth not identified by zircon Hf–O isotopes. Earth and Planetary Science Letters 456, 182–195.

Dhuime, B., Hawkesworth, C., Cawood, P., 2011. When continents formed. Science 331, 154–155.

Duchesne, J.C., Martin, H., Baginski, B., Wiszniewska, J., Vander, Auwera J., 2010. The origin of ferroan-potassic A-type granitoids: the case of the hornblende-biotite granite suite of the Mesoproterozoic Mazury complex, northeastern Poland. Canadian Mineralogist 48, 947–968.

Eiler, J.M., Crawford, A., Elliott, T.I.M., Farley, K.A., Valley, J.W., Stolper, E.M., 2000. Oxygen isotope geochemistry of oceanic-arc lavas. Journal of Petrology 41, 229–256.

Elburg, M., Jacobs, J., Andersen, T., Clark, C., Läufer, A., Ruppel, A., Krohne, N., Damaske, D., 2015. Early Neoproterozoic metagabbro-tonalite-trondhjemite of Sør Rondane (East Antarctica): implications for supercontinent assembly. Precambrian Research 259, 189–206.

Elburg, M.A., Andersen, T., Jacobs, J., Läufer, A., Ruppel, A., Krohne, N., Damaske, D., 2016. One hundred fifty million years of intrusive activity in the Sør Rondane Mountains (East Antarctica): implications for Gondwana assembly. The Journal of Geology 124, 1–26.

Elvevold, S., Engvik, A.K., 2013. Pan-African decompressional P-T path recorded by granulites from central Dronning Maud Land, Antarctica. Mineralogy and Petrology 107, 651–664.

Elvevold, S., Engvik, A.K., Abu-Alam, T.S., Myhre, P.I., Corfu, F., 2020. Prolonged high-grade metamorphism of supracrustal gneisses from Mühlig-Hofmannfjella, central Dronning Maud Land (East Antarctica). Precambrian Research 339, 105618.

Ferré, E.C., Caby, R., Peucat, J.J., Capdevila, R., Monié, P., 1998. Pan-African, post-collisional, ferro-potassic granite and quartz–monzonite plutons of Eastern Nigeria. Lithos 45, 255–279.

Fritz, H., Abdelsalam, M., Ali, K.A., Bingen, B., Collins, A.S., Fowler, A.R., Ghebreab, W., Hauzenberger, C.A., Johnson, P.R., Kusky, T.M., Macey, P., 2013. Orogen styles in the East

African Orogen: a review of the Neoproterozoic to Cambrian tectonic evolution. Journal of African Earth Sciences 86, 65–106.

Frost, B.R., Barnes, C.G., Collins, W.J., Arculus, R.J., Ellis, D.J., Frost, C.D., 2001. A geochemical classification for granitic rocks. Journal of Petrology 42, 2033–2048.

Frost, B.R., Frost, C.D., 2008. A geochemical classification for feldspathic igneous rocks. Journal of Petrology 49, 1955–1969.

Golynsky, A.V., Ferraccioli, F., Hong, J.K., Golynsky, D.A., von Frese, R.R.B., Young, D.A., Blankenship, D.D., Holt, J.W., Ivanov, S.V., Kiselev, A.V., Masolov, V.N., 2018. New magnetic anomaly map of the Antarctic. Geophysical Research Letters 45, 6437–6449.

Goodenough, K.M., Thomas, R.J., De Waele, B., Key, R.M., Schofield, D.I., Bauer, W., Tucker, R.D., Rafahatelo, J.M., Rabarimanana, M., Ralison, A.V., Randriamananjara, T., 2010. Post-collisional magmatism in the central East African Orogen: the Maevarano Suite of north Madagascar. Lithos 116, 18–34.

Grantham, G.H., Manhica, A.D.S.T., Armstrong, R.A., Kruger, F.J., Loubser, M., 2011. New SHRIMP, Rb/Sr and Sm/Nd isotope and whole rock chemical data from central Mozambique and western Dronning Maud Land, Antarctica: implications for the nature of the eastern margin of the Kalahari Craton and the amalgamation of Gondwana. Journal of African Earth Sciences 59, 74–100.

Grantham, G.H., Kramers, J.D., Eglington, B., Burger, E.P., 2019. The Ediacarian-Cambrian uplift history of western Dronning Maud Land: New ^{40}Ar-^{39}Ar and Sr/Nd data from Sverdrupfjella and Kirwanveggen, the source of the Urfjell Group and tectonic evolution of Dronning Maud Land within the Kuunga Orogeny and Gondwana amalgamation. Precambrian Research 333, 105444.

Gray, D.R., Foster, D.A., Meert, J.G., Goscombe, B.D., Armstrong, R., Trouw, R.A.J. and Passchier, C.W., 2008. A Damara orogen perspective on the assembly of southwestern Gondwana. Geological Society, London, Special Publication 294, 257–278.

Griffin, W.L., Pearson, N.J., Belousova, E., Jackson, S.E., van Achterbergh, E., O'Reilly, S.Y., Shee, S.R., 2000. The Hf isotope composition of cratonic mantle: LAM-MC-ICPMS analysis of zircon megacrysts in kimberlites. Geochimica et Cosmochimica Acta 64, 133–147.

Groenewald, P.B., Moyes, A.B., Grantham, G.H., Krynauw, J.R., 1995. East Antarctic crustal evolution: geological constraints and modelling in western Dronning Maud Land, East Antarctica. Precambrian Research 75, 231–250.

Harris, C., Le Roux, P., Cochrane, R., Martin, L., Duncan, A.R., Marsh, J.S., Le Roex, A.P., Class, C., 2015. The oxygen isotope composition of Karoo and Etendeka picrites: high δ18O mantle or crustal contamination? Contributions to Mineralogy and Petrology 170, 1–24.

Heinonen, A., Andersen, T., Rämö, O.T., Whitehouse, M., 2015. The source of Proterozoic anorthosite and rapakivi granite magmatism: evidence from combined in situ Hf – O isotopes of zircon in the Ahvenisto complex, southeastern Finland. Journal of the Geological Society 172, 103–112.

Hoch, M., Rehkämper, M., Tobschall, H.J., 2001. Sr, Nd, Pb and O isotopes of minettes from Schirmacher Oasis, East Antarctica: a case of mantle metasomatism involving subducted continental material. Journal of Petrology 42, 1387–1400.

Hoffman, J.P., 1991. Did the breakout of Laurentia turn Gondwanaland inside-out. Science 252501, 1409–1412.

Irvine, T. N. J., Baragar, W. R. A. F., 1971. A guide to the chemical classification of the common volcanic rocks. Canada Journal of Earth Science 8, 523–548.

Jacobs, J., Fanning, C.M., Henjes-Kunst, F., Olesch, M., Paech, H.J., 1998. Continuation of the Mozambique Belt into East Antarctica: Grenville age metamorphism and polyphase Pan-African high grade events in Central Dronning Maud Land. Journal of Geology 106, 385–406.

Jacobs, J., Bauer, W., Fanning, C.M., 2003a. Late Neoproterozoic/Early Palaeozoic events in central Dronning Maud Land and significance for the southern extension of the East African Orogen into East Antarctica. Precambrian Research 126, 27–53.

Jacobs, J., Klemd, R., Fanning, C.M., Bauer, W., Colombo, F., 2003b. Extensional collapse of the late Neoproterozoic-early Palaeozoic East African-Antarctic Orogen in central Dronning Maud Land, East Antarctica. Geological Society, London, Special Publication 206, 271–287.

Jacobs, J., Thomas, R. J. 2004. Himalayan-type indenter-escape tectonics model for the southern part of the late Neoproterozoic–early Paleozoic East African–Antarctic orogen. Geology 32, 721–724.

Jacobs, J., Bingen, B., Thomas, R.J., Bauer, W., Wingate, M.T., Feitio, P., 2008a. Early Palaeozoic orogenic collapse and voluminous late-tectonic magmatism in Dronning Maud Land and Mozambique: insights into the partially delaminated orogenic root of the East African–Antarctic Orogen? Geological Society, London, Special Publication 308, 69–90.

Jacobs, J., Pisarevsky, S., Thomas, R.J., Becker, T., 2008b. The Kalahari Craton during the assembly and dispersal of Rodinia. Precambrian Research 160, 142–158.

Jacobs, J., Elburg, M., Läufer, A., Kleinhanns, I.C., Henjes-Kunst, F., Estrada, S., Ruppel, A.S., Damaske, D., Montero, P., Bea, F., 2015. Two distinct Late Mesoproterozoic/Early Neoproterozoic basement provinces in central/eastern Dronning Maud Land, East Antarctica: The missing link, 15–21°E. Precambrian Research 265, 249–272.

Jacobs, J., Mikhalsky, E., Henjes-Kunst, F., Läufer, A., Thomas, R.J., Elburg, M.A., Wang, C.C., Estrada, S., Skublov, G., 2020. Neoproterozoic geodynamic evolution of easternmost Kalahari: Constraints from U-Pb-Hf-O zircon, Sm-Nd isotope and geochemical data from the Schirmacher Oasis, East Antarctica. Precambrian Research 342, 105553.

Jacobsen, S.B., Wasserburg, G.J., 1980. Sm-Nd isotopic evolution of chondrites. Earth and Planetary Science Letters 50, 139–155.

Jones, D.L., Bates, M.P., Li, Z.X., Corner, B., Hodgkinson, G., 2003. Palaeomagnetic results from the ca. 1130 Ma Borgmassivet intrusions in the Ahlmannryggen region of Dronning Maud Land, Antarctica, and tectonic implications. Tectonophysics 375, 247–260.

Kamei, A., Horie, K., Owada, M., Yuhara, M., Nakano, N., Osanai, Y., Adachi, T., Hara, Y., Terao, M., Teuchi, S., Shimura, T., 2013. Late Proterozoic juvenile arc metatonalite and adakitic intrusions in the Sør Rondane Mountains, eastern Dronning Maud Land, Antarctica. Precambrian Research 234, 47–62.

Kitano, I., Osanai, Y., Nakano, N., Adachi, T., 2016. Detrital zircon provenances for metamorphic rocks from southern Sør Rondane Mountains, East Antarctica: A new report of Archean to Mesoproterozoic zircons. Journal of Mineralogical and Petrological Sciences 111, 118–128.

Küster, D., Harms, U., 1998. Post-collisional potassic granitoids from the southern and northwestern parts of the Late Neoproterozoic East African Orogen: a review. Lithos 45, 177–195.

Laurent, O., Rapopo, M., Stevens, G., Moyen, J.-F., Martin, H., Doucelance, R., Bosq, C., 2014. Contrasting petrogenesis of Mg–K and Fe–K granitoids and implications for post-collisional magmatism: case study from the Late-Archean Matok pluton (Pietersburg block, South Africa). Lithos 196–197, 131–149.

Li, Z.L., Tainosho, Y., Kimura, J.I., Shiraishi, K., Owada, M., 2003. Pan-African alkali granitoids from the Sør Rondane Mountains, East Antarctica. Gondwana Research 6, 595–605.

Li, Z.L., Du, Z.M., Yang, S.F., Chen, H.L., Song, B., Liu, D.Y., 2006. First report of zircon SHRIMP U-Pb dating from the Dufek granite in the Sør Rondane Mountains, East Antarctica. Journal of Zhejiang University-SCIENCE A, 7, 315–319.

Li, Z.X., Bogdanova, S.V., Collins, A.S., Davidson, A., DeWaele, B., Ernst, R.E., Fitzsimons, I.C. W., Fuck, R.A., Gladkochub, D.P., Jacobs, J., Karlstrom, K.E., Lu, S., Natapov, L.M., Pease, V., Pisarevsky, S.A., Thrane, K., Vernikovsky, V., 2008. Assembly, configuration, and break- up history of Rodinia: a synthesis. Precambrian Research 160, 179–210.

Ludwig, K.R., 2011. A Geochronological Toolkit for Microsoft Excel. Berkeley Geochronology Centre Special Publications Version 4.1.

Maniar, P.D., Piccoli, P.M., 1989. Tectonic discrimination of granitoids. Geological Society of America Bulletin 101, 635–643.

Markl, G. and Henjes-Kunst F., 2004. Magmatic Conditions of Formation and Autometasomatism of Post-Kinematic Charnockites in Central Dronning Maud Land, East Antarctica: A Model of Magmatic Evolution. Geologisches Jahrbuch, Reihe B, 96, 139–185.

Marschall, H.R., Hawkesworth, C.J., Storey, C.D., Dhuime, B., Leat, P.T., Meyer, H.P., Tamm-Buckle, S., 2010. The Annandagstoppane Granite, East Antarctica: evidence for Archaean intracrustal recycling in the Kaapvaal–Grunehogna Craton from zircon O and Hf isotopes. Journal of Petrology 51, 2277–2301.

Marschall, H.R., Hawkesworth, C.J., Leat, P.T., 2013. Mesoproterozoic subduction under the eastern edge of the Kalahari-Grunehogna Craton preceding Rodinia assembly: the Ritscherflya detrital zircon record, Ahlmannryggen (Dronning Maud Land, Antarctica). Precambrian Research 236, 31–45.

Meert, J.G., Van Der Voo, R., 1997. The assembly of Gondwana 800–550 Ma. Journal of Geodynamics 23, 223–235.

Meert, J.G., 2003. A synopsis of events related to the assembly of eastern Gondwana. Tectonophysics 362, 1–40.

Merdith, A.S., Collins, A.S., Williams, S.E., Pisarevsky, S., Foden, J.D., Archibald, D.B., Blades, M.L., Alessio, B.L., Armistead, S., Plavsa, D., Clark, C., 2017. A full-plate global reconstruction of the Neoproterozoic. Gondwana Research 50, 84–134.

Middlemost, E.A., 1994. Naming materials in the magma/igneous rock system. Earth-Science Reviews 37, 215–224.

Mieth, M., Jacobs, J., Ruppel, A., Damaske, D., Läufer, A., Jokat, W., 2014. New detailed aeromagnetic and geological data of eastern Dronning Maud Land: implications for refining the tectonic and structural framework of Sør Rondane, East Antarctica. Precambrian Research 245, 174–185.

Mikhalsky, E.V., Beliatsky, B.V., Savva, E.V., Wetzel, H.U., Fedorov, L.V., Weiser, T.I., Hahne, K., 1997. Reconnaissance geochronologic data on polymetamorphic and igneous rocks of the Humboldt Mountains, central Queen Maud Land, East Antarctica. The Antarctic region: Geological evolution and processes, 45, p.53.

Miller, C.F., McDowell, S.M., Mapes, R.W., 2003. Hot and cold granites? Implications of zircon saturation temperatures and preservation of inheritance. Geology 31, 529–532.

Mole, D.R., Barnes, S.J., Taylor, R.J., Kinny, P.D., Fritz, H., 2018. A relic of the Mozambique Ocean in south-east Tanzania. Precambrian Research 305, 386–426.

Moyes, A.B., Barton, J.M., Groenewald, P.B., 1993a. Late Proterozoic to early Palaeozoic tectonism in Dronning Maud Land, Antarctica: supercontinental fragmentation and amalgamation. Journal of the Geological Society 150, 833–842.

Moyes, A.B., Groenewald, P.B., Brown, R.W., 1993b. Isotopic constraints on the age and origin of the Brattskarvet intrusive suite, Dronning Maud Land, Antarctica. Chemical Geology 106, 453–466.

Moyes, 1993. The age and origin of the Jutulsessen granitic gneiss, Gjelsvikfjella, Dronning Maud Land. South African Journal of Antarctic Research 23, 25–32.

Moyes, A.B. and Groenewald, P.B., 1996. Isotopic constraints on Pan-African metamorphism in Dronning Maud Land, Antarctica. Chemical Geology 129, 247–256.

Osanai, Y., Nogi, Y., Baba, S., Nakano, N., Adachi, T., Hokada, T., Toyoshima, T., Owada, M., Satish-Kumar, M., Kamei, A., Kitano, I., 2013. Geologic evolution of the Sør Rondane Mountains, East Antarctica: Collision tectonics proposed based on metamorphic processes and magnetic anomalies. Precambrian Research 234, 8–29.

Owada, M., Baba, S., Osanai, Y., Kagami, H., 2008. Geochemistry of post - kinematic mafic dykes from central to eastern Dronning Maud Land, East Antarctica: evidence for a Pan-African suture in Dronning Maud Land. Geological Society, London, Special Publication 308, 235–252.

Owada, M., Kamei, A., Horie, K., Shimura, T., Yuhara, M., Tsukada, K., Osanai, Y., Baba, S., 2013. Magmatic history and evolution of continental lithosphere of the Sør Rondane Mountains, eastern Dronning Maud Land, East Antarctica. Precambrian Research 234, 63–84.

Palmeri, R., Godard, G., Di Vincenzo, G., Sandroni, S., Talarico, F.M., 2018. High-pressure granulite-facies metamorphism in central Dronning Maud Land (East Antarctica): implications for Gondwana assembly. Lithos 300, 361–377.

Pant, N.C., Kundu, A., D'Souza, M.J., Saikia, A., 2013. Petrology of the Neoproterozoic granulites from Central Dronning Maud Land, East Antarctica–implications for southward extension of East African Orogen (EAO). Precambrian Research 227, 389–408.

Paulsson, O., Austrheim, H., 2003. A geochronological and geochemical study of rocks from Gjelsvikfjella, Dronning Maud Land, Antarctica—implications for Mesoproterozoic correlations and assembly of Gondwana. Precambrian Research 125, 113–138.

Pauly, J., Marschall, H.R., Meyer, H.P., Chatterjee, N., Monteleone, B., 2016. Prolonged Ediacaran–Cambrian metamorphic history and short-lived high-pressure granulite-facies metamorphism in the HU Sverdrupfjella, Dronning Maud Land (East Antarctica): evidence for continental collision during Gondwana assembly. Journal of Petrology 57, 185–228.

Peccerillo, A., Taylor, S.R., 1976. Geochemistry of Eocene calc-alkaline volcanic rocks from the Kastamonu area, northern Turkey. Contributions to mineralogy and petrology 58, 63–81.

Peck, W.H., Clechenko, C.C., Hamilton, M.A., Valley, J.W., 2010. Oxygen isotopes in the Grenville and Nain AMCG suites: Regional aspects of the crustal component in massif anorthosites. The Canadian Mineralogist 48, 763–786.

Riedel, S., Jacobs, J., Jokat, W., 2013. Interpretation of new regional aeromagnetic data over Dronning Maud Land (East Antarctica). Tectonophysics 585, 161–171.

Roland, N.W., 2004. Pan-African granite-charnockite magmatism in central Dronning Maud Land, East Antarctica: petrography, geochemistry and plate tectonic implications. Geologisches Jahrbuch, Reihe B, 96, 187–232.

Roy, S.K., Pant, N.C., Kundu, A., Dharwadkar, A., Kumar, P.K., Joshi, S., Sadiq, M., Pandey, M., 2017. Geological studies in the Baalsrudfjellet nunatak between the Schirmacher Oasis and the Wohlthat Mountains to establish the continuation of the East African Orogen (EAO) in central Dronning Maud Land, East Antarctica. Geological Society, London, Special Publication 457, 37–59.

Ruppel, A., Jacobs, J., Eagles, G., Läufer, A., Jokat, W., 2018. New geophysical data from a key region in East Antarctica: Estimates for the spatial extent of the Tonian Oceanic Arc Super Terrane (TOAST). Gondwana Research 59, 97–107.

Ruppel A., Jacobs, J., Läufer, A., Ratschbacher, L., Pfänder, J.A., Sonntag, B-L., Krasniqi, K., Elburg, M., Krohne, N., Damaske, D., Lisker, F., Protracted late Neoproterozic – early Palaeozoic deformation and cooling history of Sør Rondane, East Antarctica, from ^{40}Ar/^{39}Ar and U–Pb geochronology. Geological Magazine, in press, https://doi.org/10.1017/S0016756820000746.

Scherer, E., Münker, C., Mezger, K., 2001. Calibration of the lutetium-hafnium clock. Science 293, 683–687.

Shiraishi, K., Dunkley, D.J., Hokada, T., Fanning, C.M., Kagami, H., Hamamoto, T., 2008. Geochronological constraints on the Late Proterozoic to Cambrian crustal evolution of eastern Dronning Maud Land, East Antarctica: a synthesis of SHRIMP U-Pb age and Nd model age data. Geological Society, London, Special Publication 308, 21–67.

Söderlund, U., Patchett, P.J., Vervoort, J.D., Isachsen, C.E., 2004. The ^{176}Lu decay constant determined by Lu–Hf and U–Pb isotope systematics of Precambrian mafic intrusions. Earth and Planetary Science Letters 219, 311–324.

Stern, R.J. 1994. Arc assembly and continental collision in the Neoproterozoic East African Orogen: Implications for consolidation of Gondwanaland. Annual Review of Earth and Planetary Sciences 22, 319–351.

Stern, R.J., 2002. Crustal evolution in the East African Orogen: a neodymium isotopic perspective. Journal of African Earth Sciences 34, 109–117.

Suliman A.E., 2011. Geochronology and tectonic setting of voluminous granitoids and related rocks and associated extensional structures in Dronning Maud Land (East Antarctica). Master thesis, University of Bergen, Bergen Norway.

Tagne-Kamga, G., 2003. Petrogenesis of the Neoproterozoic Ngondo Plutonic complex (Cameroon, west central Africa): a case of late-collisional ferro-potassic magmatism. Journal of African Earth Sciences 36, 149–171.

Tsunogae, T., Dunkley, D.J., Horie, K., Endo, T., Miyamoto, T., Kato, M., 2014. Petrology and SHRIMP zircon geochronology of granulites from Vesleknausen, Lützow-Holm Complex, East Antarctica: Neoarchean magmatism and Neoproterozoic high-grade metamorphism. Geoscience Frontiers 5, 167–182.

Tsunogae, T., Yang, Q.Y., Santosh, M., 2015. Early Neoproterozoic arc magmatism in the Lützow-Holm Complex, East Antarctica: petrology, geochemistry, zircon U–Pb geochronology and Lu–Hf isotopes and tectonic implications. Precambrian Research 266, 467–489.

Ueda, K., Jacobs, J., Thomas, R.J., Kosler, J., Horstwood, M.S., Wartho, J.A., Jourdan, F., Emmel, B., Matola, R., 2012. Postcollisional high-grade metamorphism, orogenic collapse, and differential cooling of the East African Orogen of northeast Mozambique. The Journal of Geology 120, 507–530.

Valley, J.W., Kinny, P.D., Schulze, D.J., Spicuzza, M.J., 1998. Zircon megacrysts from kimberlite: oxygen isotope variability among mantle melts. Contributions to Mineralogy and Petrology 133, 1–11.

Veevers, J.J., 2007. Pan-Gondwanaland post-collisional extension marked by 650–500 Ma alkaline rocks and carbonatites and related detrital zircons: a review. Earth-Science Reviews 83, 1–47.

Viola, G., Henderson, I.H.C., Bingen, B., Thomas, R.J., Smethurst, M.D., De Azavedo, S., 2008. Growth and collapse of a deeply eroded orogen: Insights from structural, geophysical, and geochronological constraints on the Pan-African evolution of NE Mozambique. Tectonics 27, TC5009.

Von Huene, R., Scholl, D.W., 1991. Observations at convergent margins concerning sediment subduction, subduction erosion, and the growth of continental crust. Reviews of Geophysics 29, 279–316.

Wang, C.C., Jacobs, J., Elburg, M.A., Läufer, A., Thomas, R.J., Elvevold, S., 2020. Grenville-age continental arc magmatism and crustal evolution in central Dronning Maud Land (East Antarctica): Zircon geochronological and Hf-O isotopic evidence. Gondwana Research 82, 108–127.

Wareham, C.D., Pankhurst, R.J., Thomas, R.J., Storey, B.C., Grantham, G.H., Jacobs, J., Eglington, B.M., 1998. Pb, Nd, and Sr isotope mapping of Grenville-age crustal provinces in Rodinia. The Journal of Geology 106, 647–660.

Whalen, J.B., Currie, K.L., Chappell, B.W., 1987. A-type granites: geochemical characteristics, discrimination and petrogenesis. Contributions to Mineralogy and Petrology 95, 407–419.

Whitney, D.L., Evans, B.W., 2010. Abbreviations for names of rock-forming minerals. American mineralogist 95, 185–187.

Yeshanew, F.G., Pease, V., Abdelsalam, M.G., Whitehouse, M.J., 2017. Zircon U–Pb ages, $\delta^{18}O$ and whole-rock Nd isotopic compositions of the Dire Dawa Precambrian basement, eastern Ethiopia: implications for the assembly of Gondwana. Journal of the Geological Society 174, 142–156.